

# 1<sup>st</sup> AI-NanoFunc Workshop

## Advanced Microstructural Characterization of Nanomaterials

Seville 5-6 July, 2012





## Table of Content

Welcome	iii
Venue	v
Program	vii
Scientific committee	xi
Local organizing committee	xii
Abstracts Oral Presentations	
Session 1	1
Session 2	19
Session 3	29
Session 4	35
Abstracts Posters	
Session 1	43
Session 2	49
Session 3	55
Session 4	73



## Welcome

It is a great honor to organize the 1<sup>st</sup> AI-NanoFunc Workshop in "Advanced Microstructural Characterization of Nanomaterials" on July 5-6, 2012.

This two days' workshop addresses the latest advances in microstructural characterization of nanomaterials. Reflecting the main objectives and character of AI-NanoFunc project, it aims to be an open discussion forum to bring together senior and young scientists in the field.

This is the abstract book of the contributed invited and general communications that are focused in:

- new trends in advanced nanoscopies: microstructure, imaging & spectroscopies;
- application to functional materials: catalysts, nanoparticles, nanostructured coatings.

We would like to express our gratitude to all participants and invited speakers.

We are grateful to a number of organizations that funded or supported this event making it possible.

- EU FP7 capacities program REGPOT AI-NanoFunc
- Junta de Andalucía
- Instituto de Ciencia de Materiales de Sevilla CSIC-Universidad de Sevilla

Special thanks are given to those who help to prepare the 1<sup>st</sup> AI-NanoFunc workshop, specially the members of the Scientific Committee, Local Organizing Committee and the Session Chairmen, and in particular to all personnel from "Casa de la Ciencia".

**Advanced Laboratory for the NANO-analysis of Novel FUNCTIONal Materials- Team**

Asunción Fernández (Project Coordinator)

Vanda Godinho (Research manager)

Lucia Castillo (Secretary)

Rocío García (IT)



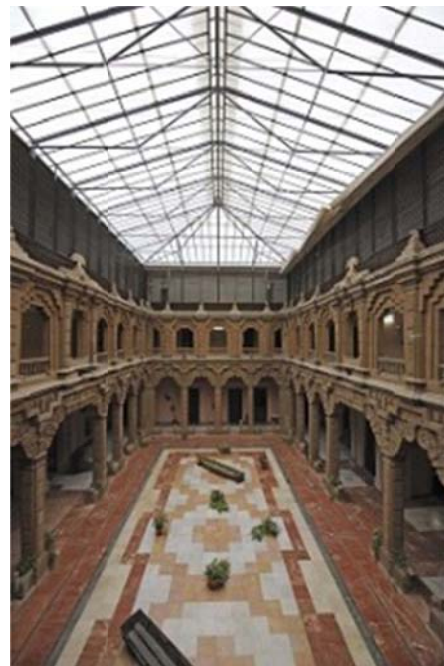
## Venue

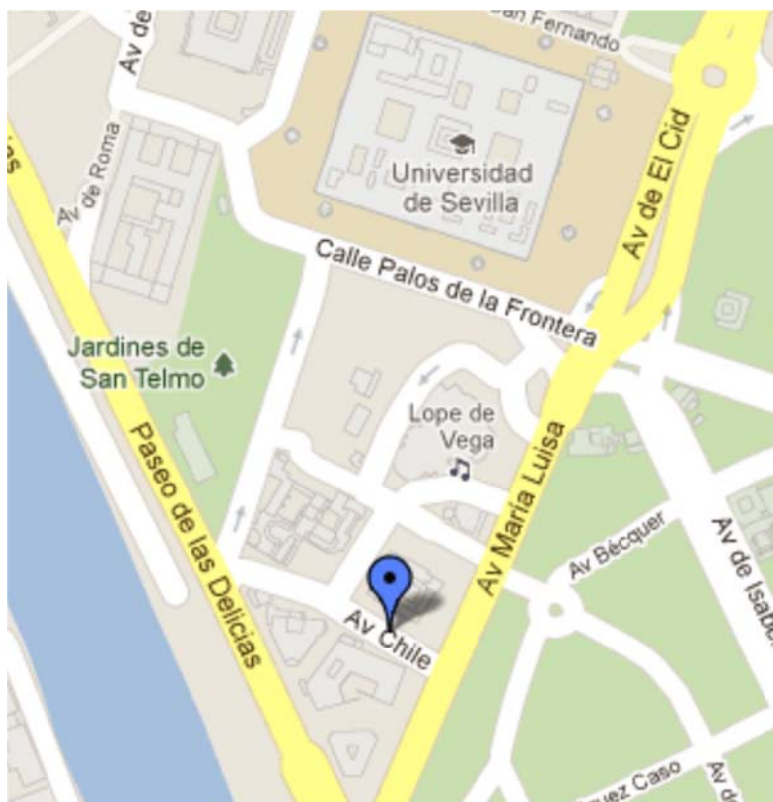
The Material Science Institute will be hosting this event in join collaboration with scientists of the network of collaborative centers in AI-NanoFunc.



The meeting will take place at the “Casa de la Ciencia” (The House of Science), placed in the historical Peruvian Pavilion from the Ibero-American Exposition of 1929. The building is a work of Manuel Piqueras Cotoí (1885 - 1937), a well-known Spanish architect born in Lucena, Córdoba. He developed most of his Career in Peru, and was the creator of important works representative of the neindigenista architecture, such as the School of Fine Arts, the Mausoleum of Pizarro in the Cathedral, and the Archiepiscopal Palace, all of them located in Lima.

At present, The House of Science shares the building with the Consulate of Peru in Seville.





Pabellón de Perú  
Av. María Luisa





## Program

Thursday 5<sup>th</sup> July

08:45-09:10	Registration
09:10-09:15	Welcome
<b>Session 1</b>	<b>New trends in advanced nanoscopies</b> L. C. Gontard; A. Kovacs
<b>09:15-09:55</b>	<b>Inv. 3D characterization of complex nanostructures</b> <b>S. Lozano-Pérez</b>
09:55-10:00	questions
10:00-10:15	<i>Applications of electron tomography to characterize the spatial distribution of nanoparticles</i> J.C. González
10:15-10:20	questions
10:20-10:35	<i>Crystal symmetry and domain structure of morphotropic PbZr<sub>1-x</sub>Ti<sub>x</sub>O<sub>3</sub>-ceramics</i> R. Schierholz
10:35-10:40	questions
10:40-10:55	<i>Determination of nanostructure and chemical composition by TEM techniques in a complex CrAl(Y)N multilayered architecture</i> T.C. Rojas
10:55-11:00	questions
11:00-11:30	coffee break
<b>11:30-12:10</b>	<b>Inv. Advanced transmission electron microscopy: structure and composition of complex oxide interfaces</b> M.Luysberg
12:10-12:15	questions
12:15-12:30	<i>Transmission electron microscopy as a tool to study defects in rock-forming minerals and high-pressure synthesised materials</i> A. Escudero
12:30-12:35	questions
12:35-12:50	<i>"An Essay on Contact Angle Measurements": Determination of Surface Roughness and Modeling of the Wetting Behavior</i> A. Terriza
12:50-12:55	questions
12:55-13:10	<i>Applications of atomic force microscopy to visualize magnetic domains and conductivity maps on the surfaces</i> C. Cerrillos
13:10-13:15	questions
13:15-15:00	lunch
<b>Session 2</b>	<b>Photonic and low dimensional nanostructures</b> T.C.Rojas; H. Miguez
<b>15:00-15:40</b>	<b>Inv. Plasma assisted fabrication of 1D supported heterostructures</b> <b>A. Borrás</b>
15:40-15:45	questions
15:45-16:00	<i>A vacuum methodology for the fabrication of hybrid core@shell nanowires based on small molecules single crystal nanowires and nanocrystalline ZnO</i> M.Macias-Montero
16:00-16:05	questions
16:05-16:20	<i>Flexible, Self-standing and Selective UV-VIS-NIR Optical Filters Based on Polymer Infiltration of Porous One Dimensional Photonic Crystals</i> M.E. Calvo
16:20-16:25	questions
16:25-16:40	<i>Photonic Crystals for Enhanced Light Harvesting in Dye Solar Cells</i> C. Lopez-Lopez
16:40-16:45	questions
16:45-17:00	<i>Modification of Mesoporous Films by Electrochemical Doping- Impact on Photocatalytic and Photovoltaic Performance</i> Jesús Idígoras
17:00-17:05	questions
17:05-19:00	poster session coffee break

Poster session

<b>Session 1</b>	<b>New trends in advaced nanoscopies</b>
P1	<i>Comparative oxidation resistance of CrAlN, CrAlYN and CrAlZrN films by electron microscopies and EELS techniques</i> T.C. Rojas, S. Domínguez-Meister, S. El Mrabet, M. Brizuela, A. García-Luis, J.C. Sánchez-López
P2	<i>Characterization of iron (III) oxide nanorods by Atomic Force Microscopy (AFM), Scanning Electronic Microscopy (SEM) and Transmission Electronic Microscopy (TEM)</i> M.V. de Paz, C. Cerrillos, F. Varela
P3	<i>Exposure of a filter feeding bivalve to gold nanoparticles: Location study by the STEM mode in a SEM-FEG microscope</i> C.A. García-Negrete, M.C. Jimenez de Haro, M. Volland, M. Hampel, J. Blasco, A. Fernández
<b>Session 2</b>	<b>Photonic and low dimensional nanostructures</b>
P1	<i>Plasma assisted fabrication of wire-on-wire organic and hybrid 1D nanostructures</i> M. Alcaire, Z. Saghi, J. C. González, A. Barranco, A. R. González-Elipe, A. Borrás
P2	<i>Light controlled patterning growth of ONWs on porous thin films</i> Y. Oulad-Zian, J. R. Sanchez-Valencia, A. Borrás, M. Coll-Bau, A. R. Gonzalez-Elipe, J. P. Espinos
P3	<i>Luminescent hybrid TiO2 nanocomposite thin films prepared by glancing angle PVD for photonic sensing</i> P. Castillero, M. Cano, J. Roales, J. R. Sánchez-Valencia, A. Barranco, A.R. González-Elipe, J.M. Pedrosa
P4	<i>Tailored luminescent emission of dyes embedded in porous resonators</i> A. Jiménez-Solano, J. M. Luque, M. E. Calvo, F. Fernández-Lázaro, H. Míguez
<b>Session 3</b>	<b>Multifunctional Nanoparticles and Nanostructures</b>
P1	<i>Correlation lengths, porosity and water adsorption in TiO<sub>2</sub> thin films prepared by glancing angle deposition</i> L. González-García, J. Parra-Barranco, J R Sánchez-Valencia, A. Barranco, A. Borrás, AR González-Elipe, M.-C. García-Gutiérrez, J.J. Hernández, DR Rueda, TA Ezquerra
P2	<i>Microstructural characterization of magnetron sputtered porous silicon coatings</i> J. Caballero-Hernandez, V. Godinho, R. Schierholz, A. Fernández
P3	<i>Metal-ceramic materials obtained by pulsed electro-erosion treatment and magnetron sputtering for medical applications</i> Y.B. Solovyeva, A.E. Kudryashov, N.A. Gloushankova, D.V. Shtansky, F.V. Kiryukhantsev-Korneev
P4	<i>Fabrication of the functionally graded metal-ceramic materials with controlled surface topography, chemistry, and wettability for bone substitution</i> I.V. Batenina, I.A. Yadroitcev, N.S. Ryashin, A.N. Sheveyko, N.A. Gloushankova, D.V. Shtansky
P5	<i>Spray pyrolysis synthesis of A-La<sub>2</sub>Si<sub>2</sub>O<sub>7</sub>: Crystal structure and luminescence</i> A.J. Fernández-Carrión, M. Ocaña and A.I. Becerro
P6	<i>Controllable synthesis and luminescence properties of GdPO<sub>4</sub> based nanophosphors</i> A. I. Becerro M. Ocaña
P7	<i>Microwave-assisted synthesis and luminescence of mesoporous Eu-doped YPO<sub>4</sub> nanophosphors with lenticular shape</i> S. Rodriguez-Liviano, F.J. Aparicio, T.C. Rojas, A. B. Hungría, L. E. Chinchilla, M. Ocaña
P8	<i>Nanoporous-Ordered Bioactive Scaffolds for Hard Tissue Engineering</i> M.L. Ramiro-Gutiérrez, A. Díaz-Cuenca
P9	<i>Biomimetic nano-mineralization of porous gelatin scaffolds for Bone Tissue-Engineering</i> S. Borrego-González, M.L. Ramiro-Gutiérrez, A. Díaz-Cuenca
<b>Session 4</b>	<b>Catalytic Materials</b>
P1	<i>Synthesis and characterization of supported Co catalyst for hydrogen generation by magnetron sputtering</i> M. Paladini, V. Godinho, G.M. Arzac, A. Fernández

Friday 6<sup>th</sup> July

<b>Session 3</b>	<b>Multifunctional Nanoparticles and Nanostructures</b>	<b>A.Fernandez; J.C.Sanchez-Lopez</b>
<b>09:30-10:10</b>	<b>Inv. Nanotechnology for life science: an example of bottom up approach, from PVD reactor to in-vivo evaluation S. Lucas</b>	
10:10-10:15	questions	
10:15-10:30	<i>TEM of hybrid Au nanoparticles capped with allylamine</i> L.C. Gontard	
10:30-10:35	questions	
10:35-10:50	<i>Nanosecond-laser control of the dichroism in supported silver nanoparticles deposited by evaporation at glancing angles</i> A. N. Filippin	
10:50-10:55	questions	
10:55-11:25	coffee break	
<b>Session 4</b>	<b>Catalytic Materials</b>	<b>A.Fernandez; J.C.Sanchez-Lopez</b>
11:25-11:40	<i>Microstructure, chemical stability and conductivity of LSM based cathodes obtained by mechanochemical method at room temperature</i> R. Moriche	
11:40-11:45	questions	
<b>11:45-12:25</b>	<b>Inv. Quantitative electron microscopy for rationalizing the activity and stability of nanocatalysts J.J.Delgado</b>	
12:25-12:30	questions	
12:30-12:45	<i>The Co-Ru-B series as catalysts for hydrogen generation: synergistic effect, chemistry and nanostructure</i> G.Arzac	
12:45-12:50	questions	
<b>12:50-13:30</b>	<b>Inv. Looking into Copper in CO-PROX Catalysts: A Multitechnique Approach G. Munuera</b>	
13:30-13:35	questions	
13:35-13:45	Closure ceremony dedicated to Prof. Guillermo Munuera in occasion of his retirement	
13:45	Farewell cocktail	



## Scientific Committee

**Agustín E. González-Elipe**

*(Instituto de Ciencia de Materiales de Sevilla)*

**Alfonso Caballero-Martinez**

*(Instituto de Ciencia de Materiales de Sevilla)*

**Asunción Fernández**

*(Instituto de Ciencia de Materiales de Sevilla)*

**María Jesús Sayagués**

*(Instituto de Ciencia de Materiales de Sevilla)*

**Rafal E. Dunin-Borkowski**

*(Ernst Ruska Center for Microscopy and Spectroscopy with Electrons)*

**Rebecca Nicholls**

*(University of Oxford Department of Materials)*

## Local Organizing Committee

**Asunción Fernández**

*(Instituto de Ciencia de Materiales de Sevilla)*

**Cristina Rojas**

*(Instituto de Ciencia de Materiales de Sevilla)*

**María del Carmen Jiménez de Haro**

*(Instituto de Ciencia de Materiales de Sevilla)*

**Lionel Cervera Gontard**

*(Instituto de Ciencia de Materiales de Sevilla)*

**Roland Schierholz**

*(Instituto de Ciencia de Materiales de Sevilla)*

**Vanda Godinho**

*(Instituto de Ciencia de Materiales de Sevilla)*

## Local secretariat

Vanda Godinho [research.manager@al-nanofunc.eu](mailto:research.manager@al-nanofunc.eu)

Lucia Castillo [secretary@al-nanofunc.eu](mailto:secretary@al-nanofunc.eu)

Rocío García [web@al-nanofunc.eu](mailto:web@al-nanofunc.eu)

## Oral presentations





## **Session 1**

### **New trends in advanced nanoscopies**



## 3D characterization of complex nanostructures

S Lozano-Perez<sup>\*a</sup>

<sup>a</sup> *Department of Materials, University of Oxford, Parks Rd, Oxford OX1 3PH, UK*

\*sergio.lozano-perez@materials.ox.ac.uk

**Keywords:** 3D, electron tomography, FIB 3D slicing

### Abstract

Many nanostructures can only be truly resolved in 3D. In the last few years, electron tomography has become a very valuable technique for this task and has allowed us to visualize nano-objects in great detail. In this presentation, the technique will be introduced and examples of application including nanoparticles [1] (see Figure 1) and corrosion intergranular crack tips [2] will be presented. In addition, when the volumes of interest are bigger, but nanometer resolution is still required, a new technique has recently become very popular: FIB 3D slicing. With the arrival of dual column FIB-SEMs and their improved level of automation, the sequential acquisition of images that can be used to reconstruct sample volumes in 3D has been enabled. This technique has been applied successfully in Oxford to the area of environmental degradation of materials in nuclear reactors, where surface oxides and localized oxidation [3] have been reconstructed and to the characterization of nanoparticles for photonic applications. Results will be presented and the techniques discussed.

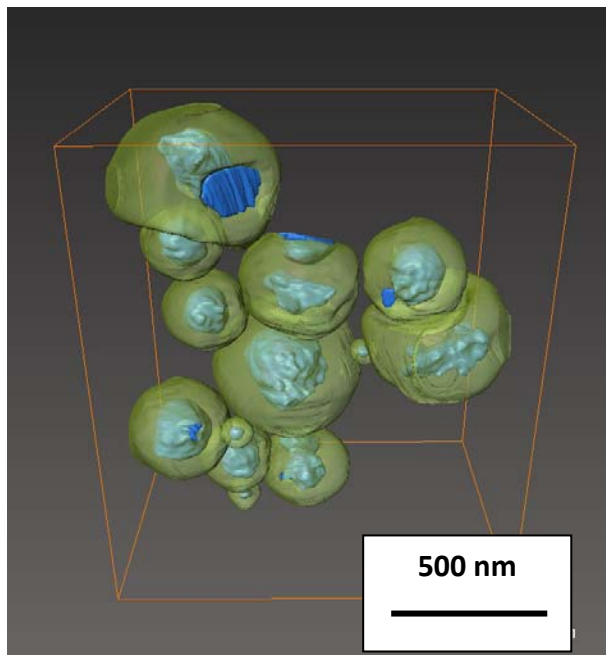


**Figure 1** – Mesoporous cerium acetate nanoparticles reconstructed in 3D by electron tomography

### References

- [1] S Shih et al., *Microscopy and Microanalysis*, **17** (2011), 54.
- [2] S Lozano-Perez et al., *J Nuclear Materials*, **408** (2011), 289.
- [3] S Lozano-Perez et al., *Corrosion Science*, **56** (2012), 78.

## Applications of Electron Tomography to Characterize the Spatial Distribution of Nanoparticles

J.C. González<sup>\*a</sup>

<sup>a</sup> *Group of Nanotechnology of Surfaces. Instituto de Ciencia de Materiales de Sevilla (CSIC-USE). Avda. Américo Vespucio 49. 41092 Seville, Spain.*

\*contact e-mail: juanc.gonzalez@icmse.csic.es

**Keywords:** electron tomography, spatial distribution, nanoparticles.

### Abstract

The demand for a quantitative description of the spatial distributions of nanoparticles will become stronger and stronger as we move into the era of nanoscience and nanotechnology, for example, by using electron tomography technique, we can quantitatively describe the variations in spatial distribution of metal or alloy nanoparticles in supported catalysts such as those used in industrial heterogeneous catalysts [1,2] or more recently in the emerging field of heterostructured organic nanowires in materials science [3,4], to characterize its hollow structure and the distribution of metal particles nanosized. We illustrate with HAADF-STEM images the applications of the advanced electron microscopy technique called electron tomography to characterize qualitative and quantitative the 3D-distribution of nanoparticles by using the nanoscale materials aforementioned.

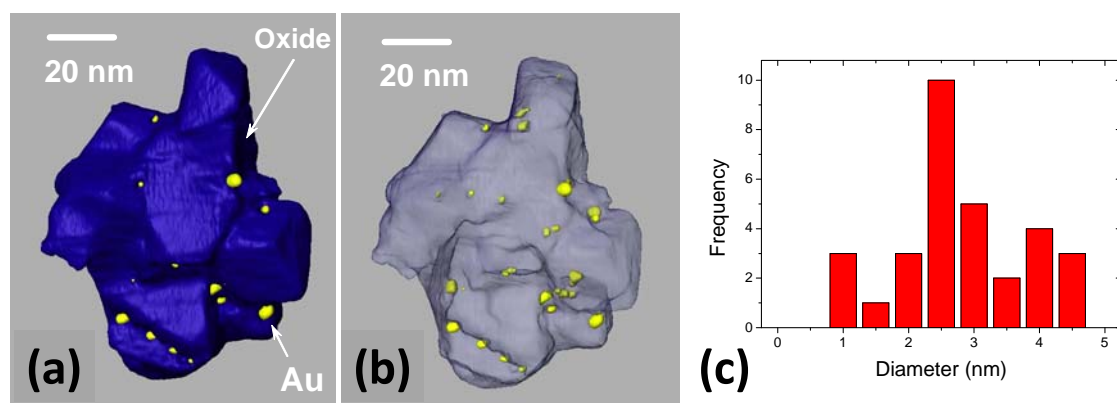


**Figure 1** – (a) Projection of tomographic reconstruction of oxidized  $\text{Au/Ce}_{0.50}\text{Zr}_{0.38}\text{Tb}_{0.12}\text{O}_{2-x}$  catalyst, (b) projection of the spatial distribution of noble metal nanoparticles over oxide support, and (c) particle size distribution of gold nanosized performed by Amira©.

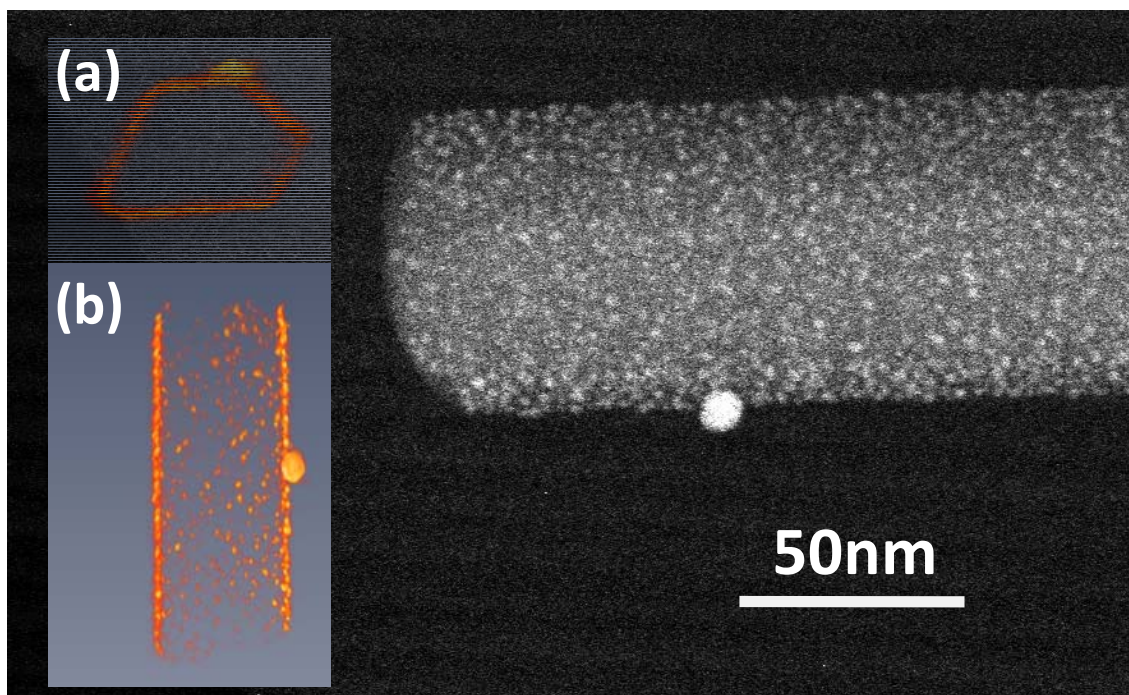


**Figure 2** – HAADF-STEM image of organic nanowire decorated with silver nanoparticles. Inset: Snapshots of *vortex* reconstruction: (a) transversal, and (b) longitudinal section by using Amira©.

## References

- [1] J.C. Gonzalez, J. C. Hernandez, M. Lopez-Haro, E. del Rio, J. J. Delgado, A. B. Hungria, S. Trasobares, S. Bernal, P. A. Midgley, and J. J. Calvino, *Angew. Chem. Int. Ed.*, **48**, (2009) 5313.
- [2] M. Lopez-Haro, K. Aboussaid, J.C. Gonzalez, Juan C. Hernandez, J.M. Pintado, G. Blanco, J.J. Calvino, P. Midgley, P. Bayle-Guillemaud, and S. Trasobares, *Chem. Mater.*, **21** (2009), 1035.
- [3] M. Alcaire, J.R. Sanchez-Valencia, F.J. Aparicio, Z. Saghi, J.C. Gonzalez A. Barranco, Y. Oulad Zian, A.R. Gonzalez-Elipe, P. Midgley, J.P. Espinos, P. Groening and A. Borrás, *Nanoscale*, **3** (2011), 4554.
- [4] M. Macias-Montero, A. Borrás, Z. Saghi, P. Romero-Gomez, J.R. Sanchez-Valencia, J.C. Gonzalez, A. Barranco, P. Midgley, J. Cotrino and A.R. Gonzalez-Elipe, *J. Mater. Chem*, **22** (2012), 1341.

## Crystal symmetry and domain structure of morphotropic $\text{PbZr}_{1-x}\text{Ti}_x\text{O}_3$ -ceramics

Roland Schierholz<sup>a</sup> and Hartmu Fues**s**<sup>b</sup>

<sup>a</sup> *Instituto de Ciencia de Materiales de Sevilla, CSIC-Uni. Sevilla, Sevilla, Spain*

<sup>b</sup> *Materialwissenschaft, TU-Darmstadt, Darmstadt, Germany*

\*contact e-mail: roland.schierholz@icmse.csic.es

**Keywords:** ferroelectrics, CBED, symmetry, TEM

### Abstract

PZT ( $\text{PbZr}_{1-x}\text{Ti}_x\text{O}_3$ ) is the most common ferroelectric material. At the morphotropic phase boundary (MPB) the piezoelectric coefficients reach their maximum values. Originally the MPB was defined as the line in the phase diagram for which the rhombohedral ( $R3m$ ) and tetragonal ( $P4mm$ ) phase coexist in equal phase fractions [1]. The excellent electromechanical properties were attributed to this coexistence until a monoclinic phase of space group symmetry  $Cm$  [2] was proposed based on x-ray diffraction. This fits because  $Cm$  is a subgroup of  $R3m$  and  $P4mm$ . But on the other hand x-ray diffraction can be affected by artifacts if the domain size is below the coherence length of the scattered radiation [3], which is typically in the range of 100 nm. Transmission electron microscopy (TEM) revealed nanodomains for those compositions, which show the reflections attributed to the monoclinic phase, so the adaptive theory [3] seems to apply.

By Convergent-Electron Beam Diffraction (CBED) the crystal symmetry of single domains can be directly probed. By this technique we were able to observe all three point group symmetries [4] and also could correlate the domain structure with the phase transitions observed in *in situ* experiments [5].

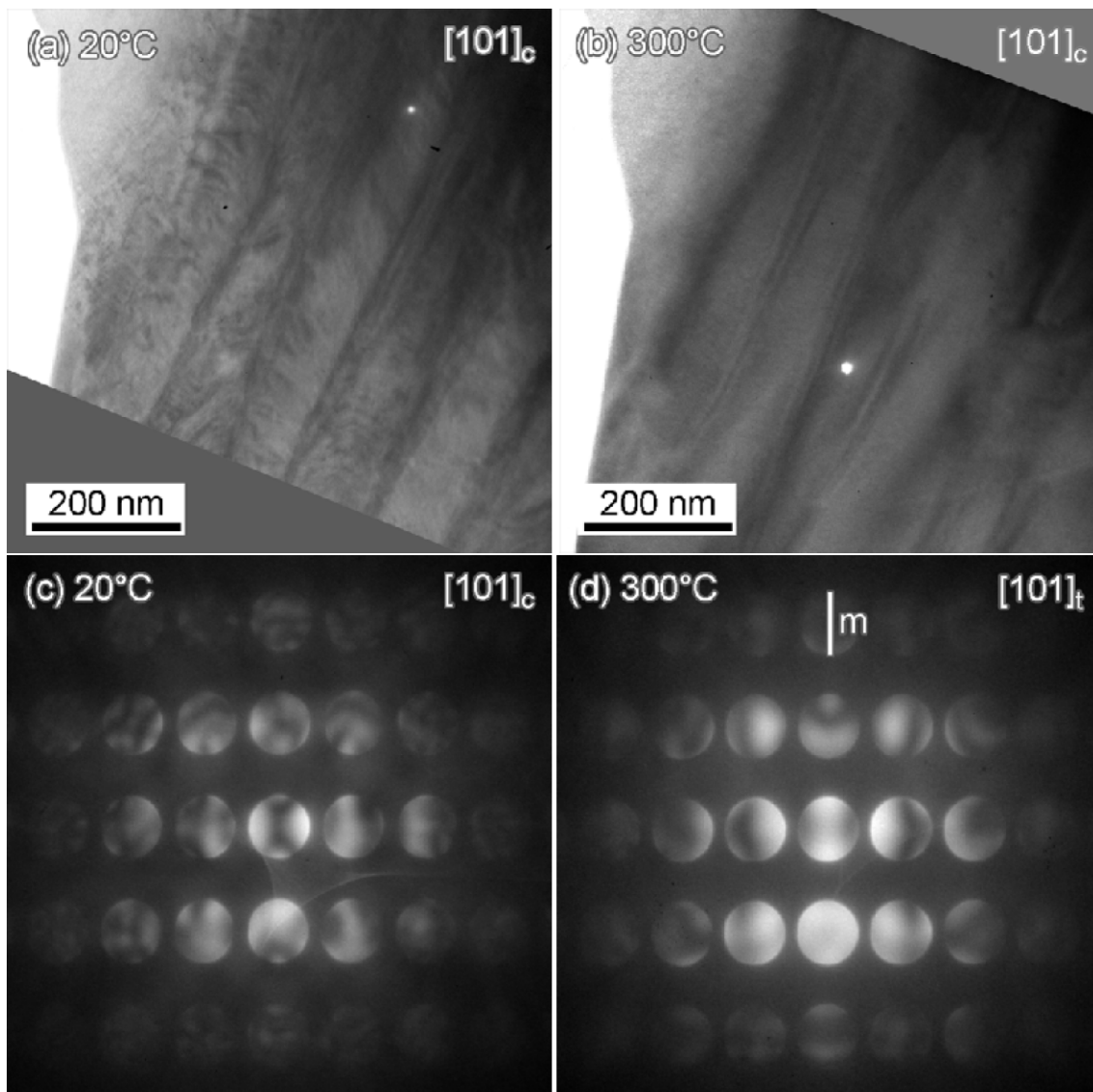


**Figure 1** – (a) Nanodomains inside microdomains at 20°C. (b) At 300°C the nanodomains disappeared while the microdomain structure is still present. (c) At 20°C no symmetry is observed in the  $[101]$  zone axis pattern. (d) At 300°C the tetragonal (010) mirror plane is present in the same domain along the same direction.

### References

- [1] Jaffe and Jaffe, Piezoelectric Ceramics, Academic Press, New York (1971).
- [2] Noheda et al. *PRB* **61** (2001) 8687-8695
- [3] Wang *PRB* **76** (2007) 024108
- [4] Schierholz and Fuess *PRB* **84** (2011) 064122
- [5] Schierholz et al. *PRB* **78** (2008) 024118.



## Determination of nanostructure and chemical composition by TEM techniques in a complex CrAl(Y)N multilayered architecture

T.C. Rojas<sup>\*a</sup>, S. Dominguez-Meister<sup>1a</sup>, M. Brizuelb<sup>b</sup>, A. García-Luis<sup>b</sup>, A. Fernández<sup>a</sup>, J.C. Sánchez-López<sup>a</sup>

<sup>a</sup> *Instituto de Ciencia de Materiales de Sevilla (CSIC-Univ. Sevilla), Avda. Américo Vespucio 49, 41092-Sevilla, Spain*

<sup>b</sup> *TECNALIA, Mikeletegui Pasealekua, 2, 20009 Donostia-San Sebastián, Spain*

\*contact e-mail:tcrojas@icmse.csic.es

**Keywords:** CrAlYN, voids, N<sub>2</sub>

### Abstract

Magnetron sputtered chromium aluminium nitride films are excellent candidates for advanced machining and protection for high temperature applications [1]. The beneficial effect of yttrium incorporation has been demonstrated by a decrease of the oxidation rate and modification of the oxide growth. We have previously reported [2] that these coatings develop a columnar microstructure constituted by a polycrystalline cubic Cr(Al)N phase, being able to withstand temperatures up to 1100°C. Inside the columns, a clear contrast formed by ordered nano-layers was also seen by transmission electron microscopy (TEM). As the mechanical properties and oxidation resistance of these coatings depend on the nanometer scale microstructure and nano-chemistry, a further and deep characterization of these nanocomposite CrAlYN coatings using nanoscale resolution electron microscopy techniques are needed to fully characterize this layered nanostructure, the present phases, and the elemental distribution at the nanoscale. Another important point is to determine the location and chemical state of Y and Al atoms inside this complex multilayer architecture.

The CrAlYN coatings have been deposited by direct current reactive magnetron sputtering on silicon substrates using metallic targets and Ar/N<sub>2</sub> mixtures under different deposition parameters (power applied to the target and rotation speed of the sample holder), to investigate their influence on the nanostructure, chemical composition, and elemental distribution by transmission electron microscopies and spectroscopic techniques: TEM, high resolution TEM (HRTEM), high angle annular dark field/scanning transmission electron microscopy (HAADF/STEM), energy dispersive X-ray (EDX) and electron energy-loss spectroscopy (EELS) spectrum images, and energy-filtered TEM (EFTEM).

In Figure 1 (left) a HAADF/STEM image of a representative sample is shown. A periodic contrast is observed formed by dark layers of ordered nanovoids of around 6-8 nm between double small dark layers with a periodicity of around 35-40nm. A high magnification bright-field TEM image of this double layer (inset (a) in the figure) demonstrates that are also formed by small pores of around 1-2 nm size. The intensity of the HAADF signal measured along the marked line supported this explanation.

Figure 1 (right) depicts the N-K and Cr-L<sub>2,3</sub> EELS spectra measured inside (A) and outside (B) of the marked pore. The shape of the N signal changes from molecular nitrogen (inside the pore) to a chromium (aluminium) nitride phase (outside). As a result, the layered contrast observed by TEM is indeed formed by nanovoids filled by molecular nitrogen. The changes of the synthesis parameters did not produce significant changes in this singular architecture but variations of the void sizes and *layer periodicity*.

The EDX and EELS elemental mappings and profiles measured on these samples using a probe of less than 1 nm, showed that the aluminum and yttrium are distributed in a sequential way following the position of the targets inside the deposition chamber. Analysis of the different atomic distribution and phases formed at the nanoscale is discussed and their influence on the oxidation resistance is also discussed.

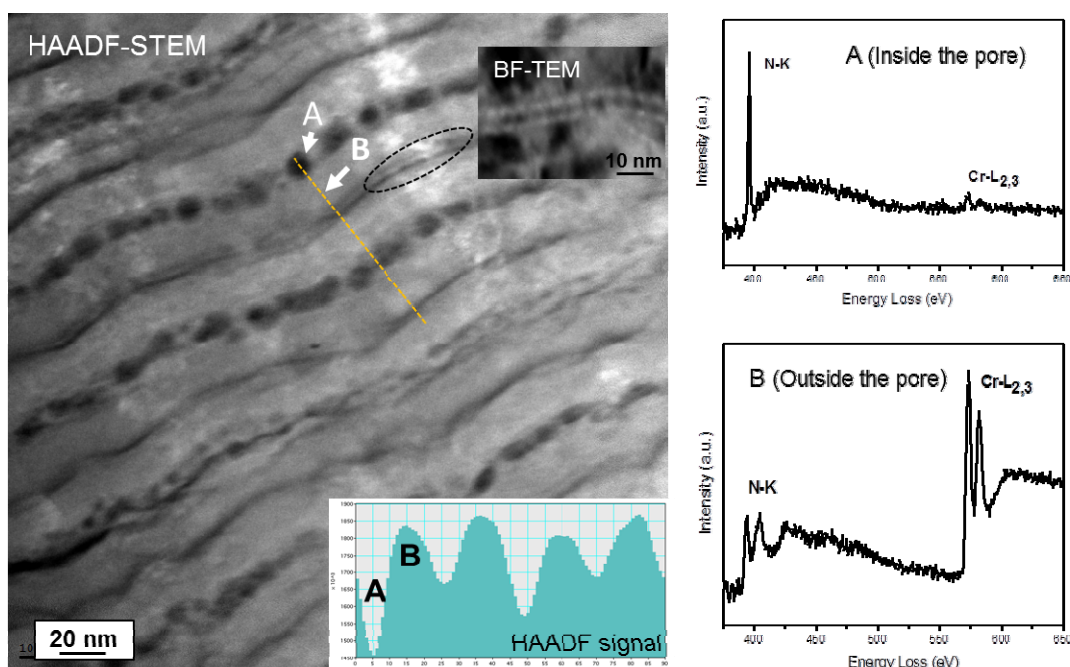


**Figure 1-** (Left) HAADF-STEM image of a CrAlYN sample. A high magnification BF-TEM image is included to show that the double layered contrast marked is formed by nanovoids of 1-2 nm. The intensity of the HAADF signal along the marked line is shown as inset. (Right) EELS spectra, N-K and Cr-L<sub>2,3</sub> edges, measured inside and outside a pore. Inside the pore the N-K edge corresponds to molecular nitrogen and outside to a nitrogen from a Cr(Al)N phase.

## References

- [1] J. Lin, B. Mishra, J.J. Moore, W.D. Sproul, Surf. Coat. Technol. **202** (2008) 3272.
- [2] T.C. Rojas, S. El Mrabet, S. Domínguez-Meister, M. Brizuela, A. García-Luis, J.C. Sánchez-López. Surf. Coat. Technol. (2012) in press.
- [3] The authors gratefully acknowledge funding from the European Union (Al-Nanofunc project REGPOT-CT-2011-285895), Spanish MEC (MAT2011-29074-C02-01/02) and CSIC (201060I041).

## Advanced transmission electron microscopy: Structure and composition of complex oxide interfaces

M. Luysberg<sup>1\*</sup>, J. Schubert<sup>2</sup>, K. Rahmanizadeh<sup>3</sup>, G. Bihlmayer<sup>3</sup>, L. Fitting Kourkoutis<sup>4</sup>,  
and D. A. Muller<sup>4</sup>

<sup>1</sup> Peter Grünberg Institute 5 and Ernst Ruska-Centre for Microscopy and Spectroscopy  
with Electrons, Research Centre Jülich, 52425 Jülich, Germany

<sup>2</sup> Peter Grünberg Institute 9, Research Centre Jülich, 52425 Jülich, Germany

<sup>3</sup> Peter Grünberg Institute 1, Research Centre Jülich, 52425 Jülich, Germany

<sup>4</sup> School of Applied and Engineering Physics, Cornell University, Ithaca, USA

\*m.luysberg@fz-juelich.de

**Keywords:** STEM/EELS, complex oxides, high-resolution STEM

### Abstract

The advent of aberration correctors for electron lenses in the transmission electron microscope in conjunction with state of the art electron spectrometers allows for measurements of structure and composition on the atomic scale. The talk highlights these achievements on one example: the structure and composition of scandate/titanate interfaces.

Unlike the polar interface between  $\text{LaAlO}_3$  and  $\text{SrTiO}_3$ , where a conducting interface has been discovered [1], the polar  $\text{DyScO}_3/\text{SrTiO}_3$  system remains electrically insulating. This can be attributed to an off-stoichiometry of ions of different valence at the interface between e.g.  $\text{DyScO}_3$  and  $\text{SrTiO}_3$ , which counteracts the interface dipoles arising from the polar discontinuity [2]. This off-stoichiometry is experimentally measured by high-resolution scanning transmission electron microscopy and atomic-resolution electron energy loss spectroscopy as well as predicted by ab-initio calculations [3]. Figure 1 displays the result of ab initio calculations of the  $\text{DyScO}_3/\text{SrTiO}_3$  interface [2], where a mixed Ti/Sc or Sr/Dy interface is introduced. Clearly, for all atomic layers a well defined band gap occurs, which implies the interface being electrically insulating.

The minimum energy configuration involves an ordered interface, where individual, neighbored atom columns along the interface are alternating occupied with Sr and Dy atoms. This theoretical result agrees with our experimental observations: Figure 2 displays spectroscopic imaging of a  $\text{DyScO}_3$  layer embedded in  $\text{SrTiO}_3$ , which is located at the top and bottom. The spectroscopic maps were evaluated from electron energy loss spectra measured at every pixel. The high-angle annular dark field image shown on the left was acquired simultaneously with the spectroscopic data. At the interface an ordered structure is revealed with every second atom column appearing brighter than its neighbour (see the arrows in Fig. 2). This ordering is also seen in the Dy map, suggesting that every second atomic column along the interface consists mostly of Dy. In contrast, the spectroscopic maps of Ti and Sc do not show systematic variations in composition. In agreement with our previous investigations [2], an intermixing extending over about two monolayers is observed.

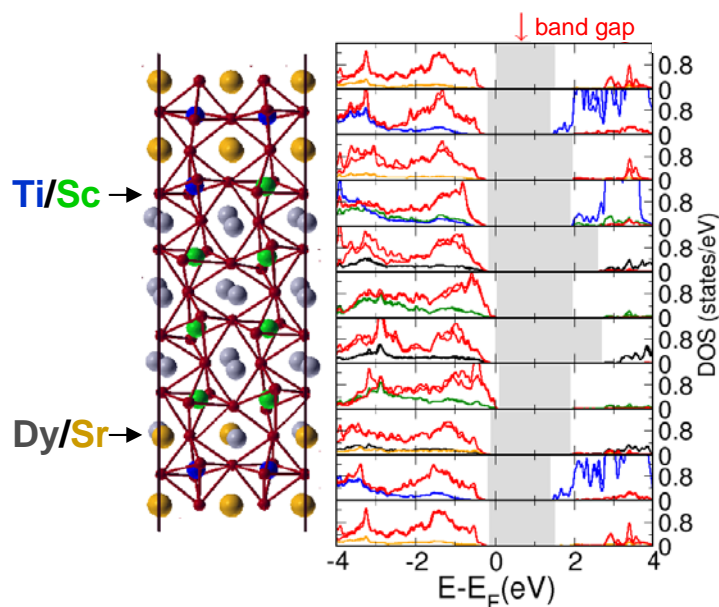


**Figure 1.** Minimum energy configuration of a SrTiO<sub>3</sub>/DyScO<sub>3</sub>/SrTiO<sub>3</sub> supercell obtained by DFT calculations. DyScO<sub>3</sub> is viewed along the [010] and SrTiO<sub>3</sub> along the [001] direction. The band structure shown on the right hand side reveals a well defined band gap for all lattice planes. Colour codes for labelling different atomic species are the same within both images (red: O, blue: Ti, gold: Sr, green: Sc, silver: Dy).

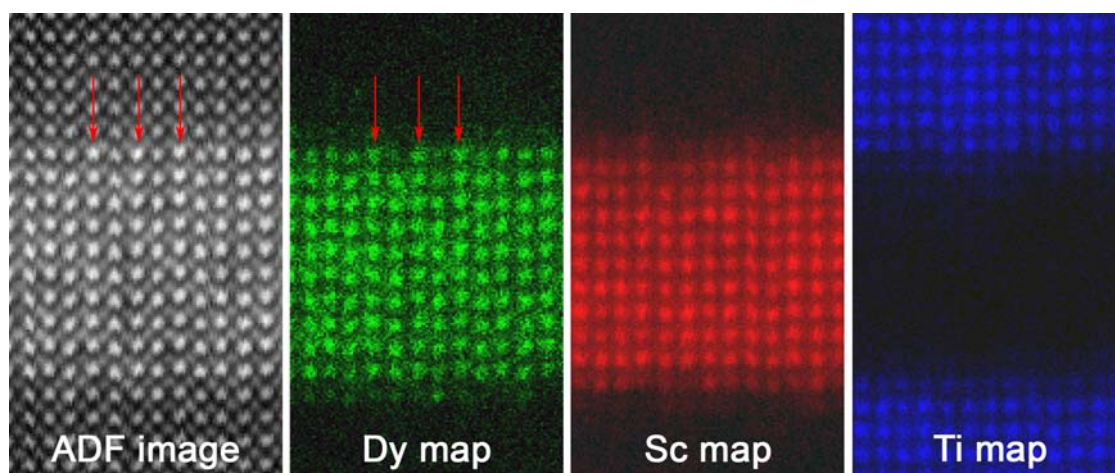


**Figure 2.** Spectroscopic imaging of DyScO<sub>3</sub> embedded in SrTiO<sub>3</sub> corrected for specimen drift, acquired with a NION UltraSTEM 100 (accelerating voltage 100kV, convergence angle: 25 mrad, collection angle: 77 mrad, probe size: 0.1 nm). DyScO<sub>3</sub> is viewed along the [101] direction and SrTiO<sub>3</sub> along the [010] direction, the width of the images is 4.9 nm. The high-angle annular dark field image (ADF image) is recorded simultaneously with the spectroscopy data. Arrows denote atomic columns of brighter contrast within the interface plane. The Dy M<sub>4,5</sub>-map (1296 eV) reveals interfacial ordering, whereas no ordering effect is observed in the Sc L<sub>2,3</sub>-map (401 eV) and the Ti L<sub>2,3</sub>-map (456 eV).

### References

- [1] N. Nakagawa, H-Y. Hwang, and D. A. Muller, *Nature Materials* **5** (2006), 204..
- [2] M. Luysberg, M. Heidelmann, L. Houben, M. Boese, T. Heeg, J. Schubert, and M. Roeckerath *Acta Materialia* **57** (2009), 3192
- [3] K. Rahmanizadeh, G. Bihlmayer, M. Luysberg, and S. Blügel *Phys. Rev.* **B 85**, (2012), 075314

## Transmission Electron Microscopy as a tool to study defects in rock-forming minerals and high-pressure synthesised materials

Alberto Escudero<sup>1\*</sup> and Falko Langenhorst<sup>2</sup>

<sup>1</sup> Instituto de Ciencia de Materiales de Sevilla. CSIC-Universidad de Sevilla, Spain

<sup>2</sup> Institut für Geowissenschaften, Friedrich-Schiller-Universität Jena, Jena, Germany

\*contact e-mail: aescudero@icmse.csic.es

**Keywords:** defects, dislocations, twins boundaries, stacking faults

### Abstract

In a real material structure there are always some local violations or defects in the perfect arrangement of the ideal crystal structure. Defects are not only responsible for some properties of the materials, such as reactivity or colour, but they can also provide useful information about the history of the material and the existence of phase transitions. This is especially relevant in rock-forming minerals and in materials synthesised at high pressure. Transmission Electron Microscopy is an appropriate characterization technique to study the defects in both systems. Some examples of defects observed in both natural and synthesised minerals will be shown, explaining their implications.

Titanium dioxide ( $\text{TiO}_2$ ) is intensively studied due to both basic and applied interests in geology and material science. Rutile is a common accessory mineral in metamorphic and igneous rocks. Rutile transforms to high-pressure  $\text{TiO}_2$  polymorphs with the structure of  $\alpha\text{-PbO}_2$  and  $\text{ZrO}_2$  baddeleyite. The presence of high pressure polymorphs of  $\text{TiO}_2$  as well as the defect microstructure of rutile grains that have experienced both high-pressure and high-temperature conditions can be used to estimate metamorphic peak conditions and to describe possible high-pressure and deformation conditions of rutile bearing ultra-high pressure metamorphic rocks. We have observed different defects in natural  $\text{TiO}_2$  rutile grains from diamondiferous gneiss of the Saxonian Erzgebirge, Germany, a well-known ultra-high pressure metamorphic terrane. Defects such as ilmenite exolutions, dislocations and subgrain boundaries have mineralogical implications in the history of these rocks [1].

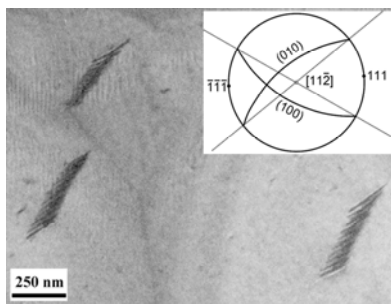


**Figure 1** – Bright field TEM image of a rutile inclusion in garnet showing three dislocations decorated with ilmenite needles.

Defects in materials synthesised in the laboratory at high pressure and high temperature also provide useful information on high pressure phase transitions. For example, an orthorhombic  $\text{CaCl}_2$  type structure has been observed for the first time in both recovered Al- and Cr- doped  $\text{TiO}_2$  grains quenched from high pressure. Such a phase transformation is reflected in a  $\text{TiO}_2$  microstructure consisting of (110) twins, and has also important implications in mineralogy [2]. Further phase transitions in the  $\text{TiO}_2$  system take place at higher pressures. A polymorph with the structure of  $\text{ZrO}_2$  baddeleyite is expected at pressures above 17 GPa, but such polymorph is not observed in the recovered samples. The observation of  $\alpha\text{-PbO}_2$  structured  $\text{TiO}_2$  grains decorated with  $\pi$  fringes stacking faults indicates that the phase transition to the  $\text{ZrO}_2$  baddeleyite takes place with increasing the synthesis pressure. However, such structure is non-quenchable and reverts to  $\alpha\text{-PbO}_2$  structured  $\text{TiO}_2$  when releasing the pressure [3].

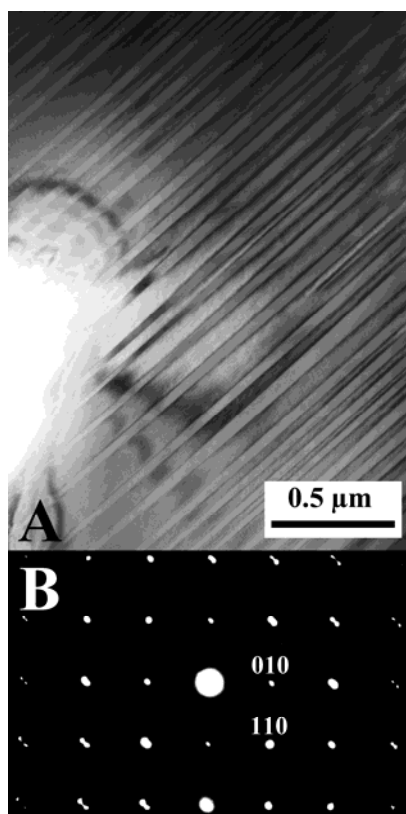


**Figure 2** – (a) Bright-field TEM micrograph of an Al-doped  $\text{CaCl}_2$  type  $\text{TiO}_2$  grain in the sample synthesized at 6 GPa and 1300 °C, showing a microstructure consisting of twins. (b) Electron diffraction pattern zone axis [001].

### References

- [1] Escudero, A.; Miyajima, N.; Langenhorst, F., *Chemie der Erde – Geochemistry*, **72** (2012), 25-30.
- [2] Escudero, A.; Langenhorst, F.; Müller, W. F. *American Mineralogist*, (2012) doi: 10.2138/am.2012.4049.
- [3] Escudero, A.; Langenhorst, F., *Physics of the Earth and Planetary Interiors*, **190-191** (2012), 87-94.

## “An Essay on Contact Angle Measurements”: Determination of Surface Roughness and Modeling of the Wetting Behavior

A. Terriza<sup>\*</sup>, Rafael Alvarez, Francisco Yubero, Ana Borrás and Agustín R. González-Elípe

ICMS, Avda. Américo Vespucio 49, 41092 Sevilla, Spain

\*contact email: antonia.terriza@icmse.csic.es

### Keywords:

### Abstract

The problem of determining surface roughness values and their use to assess the wetting behavior of surfaces has been studied. For very rough surfaces it is shown that depending on the observation scale by atomic force microscopy (AFM) quite different RMS roughness values can be obtained and that only the values taken at saturation can be used for properly describing the roughness of the examined materials. This effect has clear consequences when trying to apply wetting models to account for the influence of roughness on contact angles. These ideas are discussed with examples taken from rough polymer surfaces subjected to plasma etching.

In previous articles it has been stressed the need to use dynamic measurements to properly characterize the wetting properties of a given surface.[1–3]. In addition, the influence of surface roughness in the measurement of contact angles (CAs) and into the CA hysteresis when measuring advancing and receding angles by goniometry has been reported [2]. Many times surface roughness is determined by means of atomic force microscopy (AFM) under the implicit idea that a particular surface is characterized by just one RMS roughness value. However, such an assumption is not sustained by either the empirical evidence [4] or by the principles of the so-called Dynamic Scaling Theory (DST) applied to describe surface growth processes.[5,6]. It is an experimental result and a theoretical conclusion from the DST that the measured RMS roughness values depend on the scale of measurement and the more correct RMS roughness value is obtained when the surface has reached its “saturation.” We applied the model of Wenzel,[7] to relate the surface roughness and CAs of real surfaces and determine the actual threshold observation area for which the surface roughness is properly calculated.

“A. Terriza et al, *Plasma Processes and Polymers*, **8** (2011), 998”

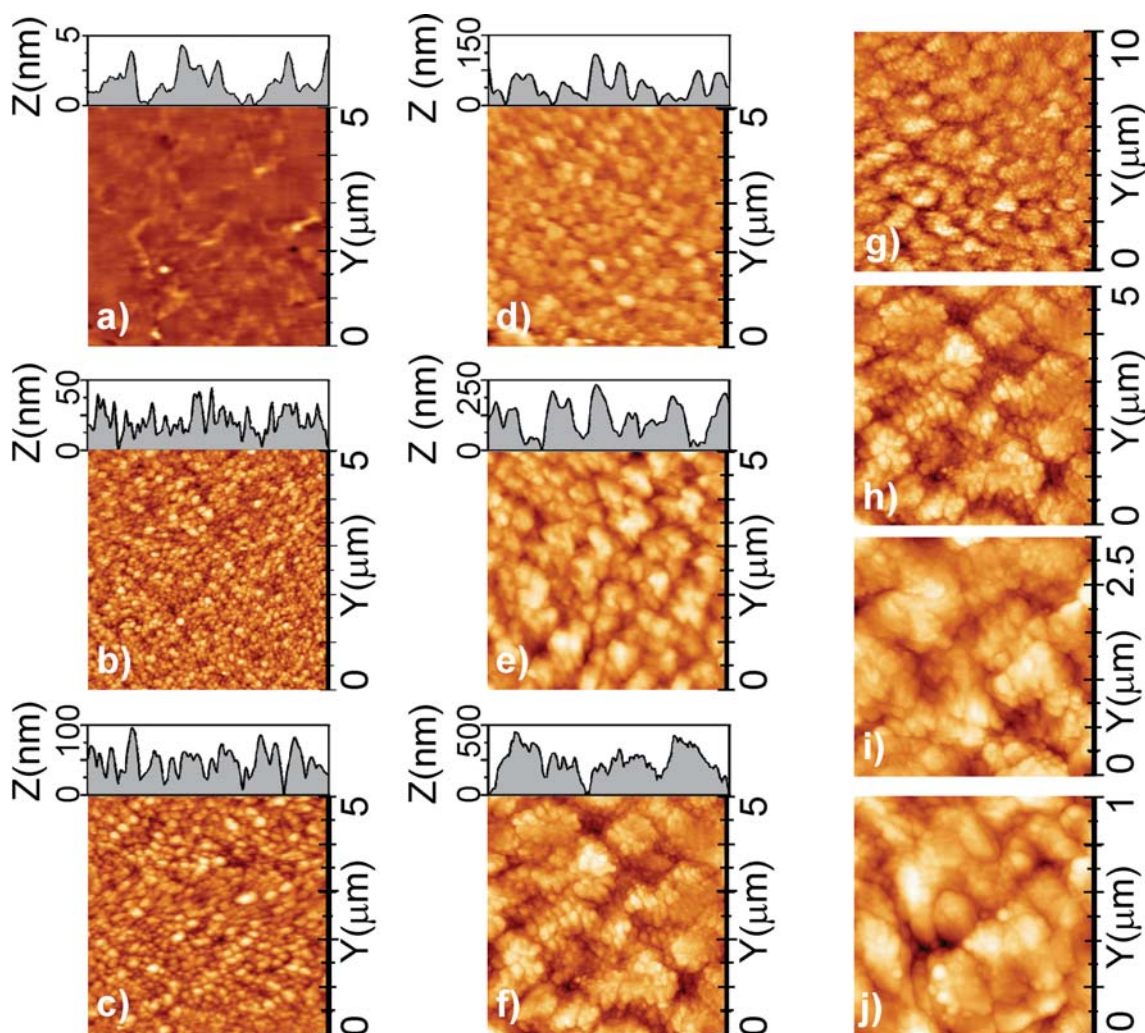


**Figure 1** –  $5\mu\text{m} \times 5\mu\text{m}$  AFM images and line scans of the PET samples subjected to oxygen plasma etching for increasing periods of time: (a) original sample; (b) 10 min; (c) 15 min; (d) 20 min; (e) 30 min; (f) 45 min; (g–j) AFM Images of the PET sample subjected to oxygen etching for 45 min taken over scanning areas of  $1\mu\text{m} \times 1\mu\text{m}$ ,  $2.5\mu\text{m} \times 2.5\mu\text{m}$ ,  $5\mu\text{m} \times 5\mu\text{m}$  and  $10\mu\text{m} \times 10\mu\text{m}$ .

## References

- [1] M. Strobel, Ch. S. Lyons, *Plasma Processes and Polymers*, **8** (2011), 8.
- [2] R. Di Mundo, F. Palumbo, *Plasma Processes and Polymers*, **8** (2011), 14.
- [3] M. Müller, Oehr. Ch, *Plasma Processes and Polymers*, **8** (2011), 19.
- [4] A. Borrás, A. Yanguas/Gil, A. Barranco, J. Cotrino, A. R. González-Elipe, *Physical Review B*, **76** (2007), 76.
- [5] A.-L. Barabási, H. E. Stanley, “*Fractal Concepts in Surface Growth*”, Cambridge University Press, Cambridge, (2011).
- [6] M. Pelliccione, T.-M. Lu, “*Evolution of Thin Films Morphology. Modelling and Simulations*”, Springer Verlag, Heidelberg, (2008).
- [7] R. N. Wenzel, *Industrial and Engineering Chemistry*, **28** (1936), 988.



## Applications of Atomic Force Microscopy to visualize magnetic domains and conductivity maps on the surfaces

C. Cerrillos <sup>\*a</sup> and F. Varela <sup>a</sup>

<sup>a</sup> *Centro de Investigación, Tecnología e Innovación de la Universidad de Sevilla, Avda. Reina Mercedes 4-b, 41012 Sevilla, Spain.*

\*contact e-mail: ccerrillos@us.es

**Keywords:** AFM, MFM, CS-AFM and photovoltaic materials.

### Abstract

The Scanning Probe Microscopy (SPM) provides three-dimensional, real-space images of surfaces at high spatial resolution. Images are based on detecting the local interaction between a small probe tip and a surface. Depending on the particular SPM, the images can represent physical surface topography, electronic structure, electric or magnetic fields, or a number of other local properties.

In the case of MFM [1], the interaction is the static-magnetic force between the tip (covered to the ferromagnetic material) and the surfaces. This long-range forces act in addition to short-range forces between two surfaces. Close to the surface, these forces are much smaller than those due to van der Waals interactions and usually contribute little to the signal. Further from the surface, the van der Waals interaction decay rapidly to the point of being negligible. In this regime, long-range forces are still significant. The difference in decay length provides a means to distinguish the two types of interactions. The general relations describing the force experienced by a tip above a homogeneous surface for magnetic interaction is described in the following equation:

$$F_{magnetostatic} = \nabla(m \bullet B_{sample})$$

$B_{sample}$  is the magnetic field emanating from the sample surface, and  $m$  is the magnetic dipole of the tip.

The following figure (Figure 1 - ) show the topography and the magnetic domains images of hard disk sample.

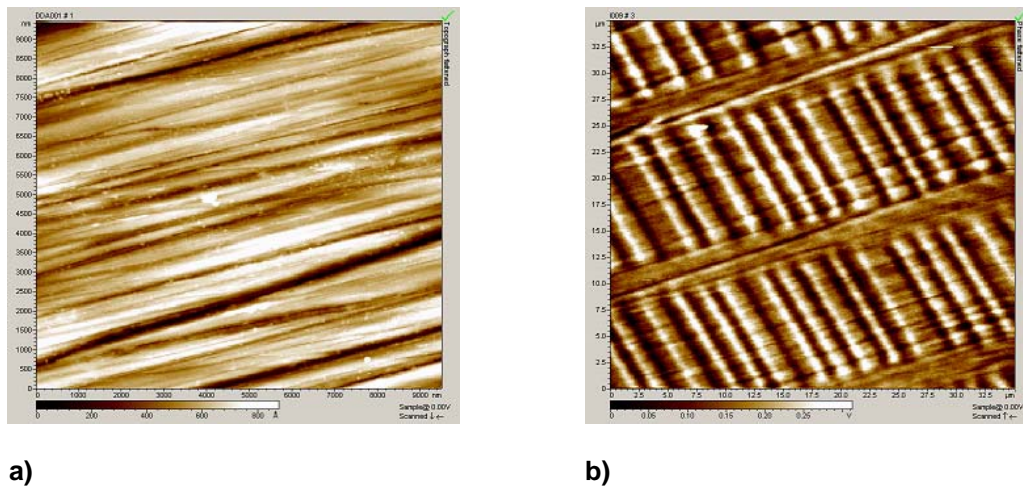


**Figure 1** – Topography and magnetic domains images of hard disk (a, b) sample obtained using MFM.

In the case of Current Sensing AFM (Figure 2 - ), the principles are:

- A bias is applied to the sample; current flows through the conducting cantilever to preamp.
- Allows simultaneous probing of conductivity and topography.

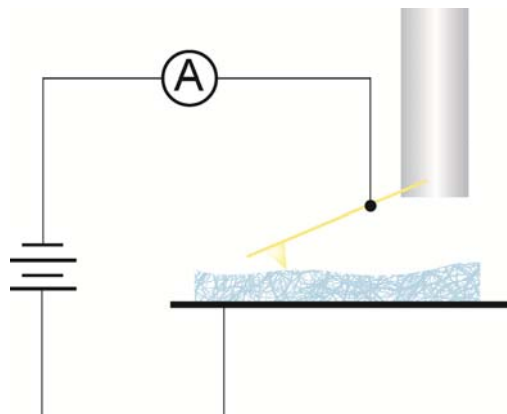


**Figure 2** – Current sensing-AFM

Current sensing AFM (CS-AFM), also known as conducting AFM, is a powerful technique for the characterization of photovoltaic materials [2-4]. Indium tin oxide (ITO) is an example of transparent conductive oxide (TCO), which plays a very important role in photovoltaic cells, and It is widely used in organic solar devices as the supporting substrate [5].

The topography and the current images of ITO are represented in the following figure (Figure 3- ).

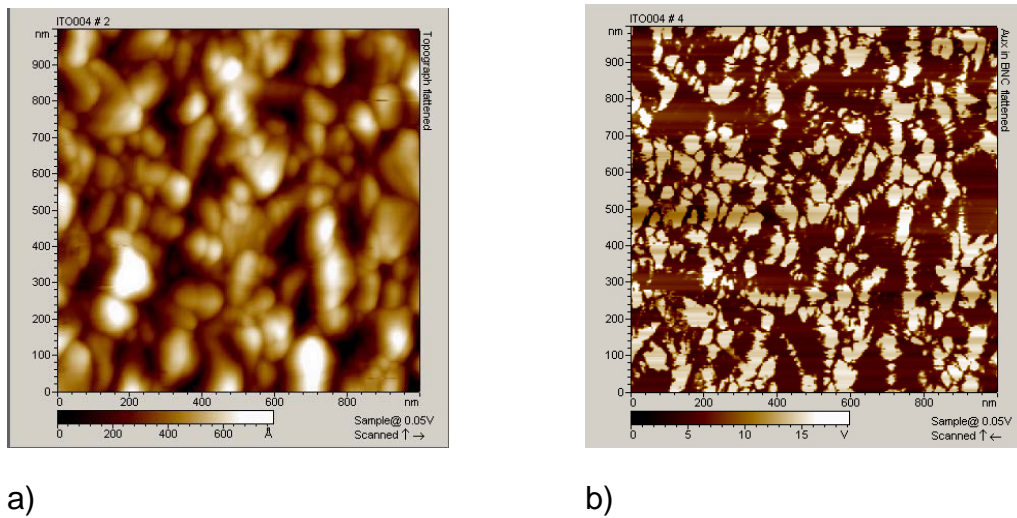


**Figure 3** – Topography and conductivity domains of Indium tin oxide (ITO) obtained using CS-AFM.

### References

- [1] Bonnell D, *Scanning Probe Microscopy and Spectroscopy*, John Wiley & Sons, (2001).
- [2] Rezek B, Stuchlyk J, Fejfar A and Kocka, *Appl. Phys. Lett.*, **74** (1999), 1475.
- [3] Azulay D, Balberg I, Chu V, Conde JP and Milo, *Phys Rev. B*, **71** (2005), 113304.
- [4] Cavallini A, *Microscopy of Semiconducting Materials*, (2007), 301-304.
- [5] Chahyung K, Bongki L, Hee J. Y, Hyun M. L, Jae G. L and Hyunjung S, *Journal of the Korean Physical Society*, **47** (2005), S417.



## **Session 2**

### **Photonic and low dimensional nanostructures**



## Plasma assisted fabrication of 1D supported heterostructures

Ana Borrás

*Nanotechnology on Surfaces Lab. Materials Science Institute of Seville (CSIC-US) C/  
Americo Vesputio 49, 41092, Seville (Spain)*

\*contact e-mail: [anaisabel.borras@icmse.csic.es](mailto:anaisabel.borras@icmse.csic.es)

**Keywords:** organic nanowire, hybrid, hierarchical, TiO<sub>2</sub>, ZnO

### Abstract

Plasma methods have been widely used in the fabrication of carbon nanotubes and nanofibres and semiconducting inorganic nanowires. A natural progression of the research in the field of 1D nanostructures is the synthesis of multicomponent nanowires and nanofibres [1]. In this communication we present recent advances in the fabrication by plasma and plasma assisted methods of 1D supported heterostructures. Perspectives and potential applications of the 1D nanostructures in solar cells, multisensors and microfluidics and their controlled fabrication on processable substrates will be discussed. As examples of these nanomaterials we will show the formation of:

- i) Heterostructured metal/metal oxide nanorods by plasma enhanced chemical vapor deposition of organo-metal precursors (TTIP for TiO<sub>2</sub> and DEZ for ZnO) on metal NPs acting as seeds [2]. In the particular case of the Ag@ZnO NRs, the characterization of individual NRs by HAADF-STEM allows to elucidate their inner structure: a hollow ZnO shell decorated with silver NPs [3]. The formation of zig-zag structures will be also presented.
- ii) Hierarchical organic nanowires by combination of physical vapor deposition of single crystal organic nanowires (ONWs) with soft plasma etching. In this case, the pristine surface of the ONWs based on porphyrin, phthalocyanine and perylene is slightly modified by oxygen plasma. The induced roughness act as nucleation centers for the formation of new organic nanowires resulting in hierarchical and/or heterostructured nanotrees conformations [4, 5].
- iii) Hybrid nanowires fabricated by soft plasma processing at different temperatures of metal-organic NWs (based on metal-porphyrins and metal-phthalocyanines)
- iv) Core@shell organic and hybrid nanowires. The unprecedented use of PECVD for the fabrication of conformal layers on organic nanowires is demonstrated for organic@organic and organic@inorganic configurations.

### References

- [1] A. Borrás, M. Macias-Montero, P. Romero-Gomez and A. R. Gonzalez-Elipe *J. Phys. D: Appl. Phys.* **44** (2011) 174016.
- [2] A. Borrás, A. Barranco, F. Yubero and A. R. Gonzalez-Elipe *Nanotechnol.* **17** (2006) 3518.
- [3] M. Macias-Montero, A. Borrás, Z. Saghi, P. Romero-Gomez, J. R. Sanchez-Valencia, J. C. Gonzalez, A. Barranco, P. Midgley, J. Cotrino and A. R. Gonzalez-Elipe *J. Mater. Chem.* **22** (2012) 1341.

- [4] A. Borrás, M. Aguirre, C. Lopez-Cartes, O. Groening and P. Groening *Chem. Mater.* **20** (2008) 7371-7373.
- [5] M. Alcaire, J. R. Sanchez-Valencia, F. J. Aparicio, Z. Saghi, J. C. Gonzalez-Gonzalez, A. Barranco, Y. Oulad-Zian, A. R. Gonzalez-Elipe, P. Midgley, J. P. Espinos, P. Groening and A. Borrás *Nanoscale* **3** (2011) 4554-4559.



## A vacuum methodology for the fabrication of hybrid core@shell nanowires based on small molecules single crystal nanowires and nanocrystalline ZnO

Manuel Macias-Montero,<sup>1</sup> A. Nicolas Filippin,<sup>1</sup> Zineb Saghi,<sup>2,3</sup> Juan C. Gonzalez,<sup>1</sup> Angel Barranco,<sup>1</sup> Agustin R. González-Elipse<sup>1</sup> and Ana Borrás<sup>1\*</sup>

<sup>1</sup> Instituto de Ciencia de Materiales de Sevilla (ICMS, CSIC-US), Nanotechnology on Surfaces Lab., C/ Américo Vespucio 49, 41092, Sevilla, Spain.

<sup>2</sup> Department of Materials Science and Metallurgy, University of Cambridge, Pembroke Street, CB2 3QZ, Cambridge, United Kingdom.

<sup>3</sup> Fundación Progreso y Salud BIONAND C/ Severo Ochoa 35, Parque Tecnológico de Andalucía, 29590 Malaga, Spain.

\*contact e-mail: [anaisabel.borras@icmse.csic.es](mailto:anaisabel.borras@icmse.csic.es), [manuel.macias@icmse.csic.es](mailto:manuel.macias@icmse.csic.es)

**Keywords:** hybrid nanostructures, organic nanowires, ZnO, core@shell nanocrystalline, wideband fluorescent emission.

### Abstract

In this communication we show the unprecedented fabrication of hybrid core@shell nanowires formed by an inner organic nanowire surrounded by a nanocrystalline ZnO layer. Single crystal organic nanowires made of small-molecules such as metal porphyrins, metal phthalocyanines and perylenes are fabricated by physical vapor deposition on metal and oxide substrates of tailored microstructure [1]. The conformal growth of the ZnO layer at low temperature by plasma enhanced chemical vapor deposition allows the formation of the complex heterostructures keeping untouched the organic crystal structure as demonstrated by HRTEM and SAED. As result, multifunctional hybrid core@shell architectures are fabricated on processable substrates. Examples of wave guiding and wide range fluorescent emission of porphyrins@ZnO and perylene@ZnO nanostructures are shown.

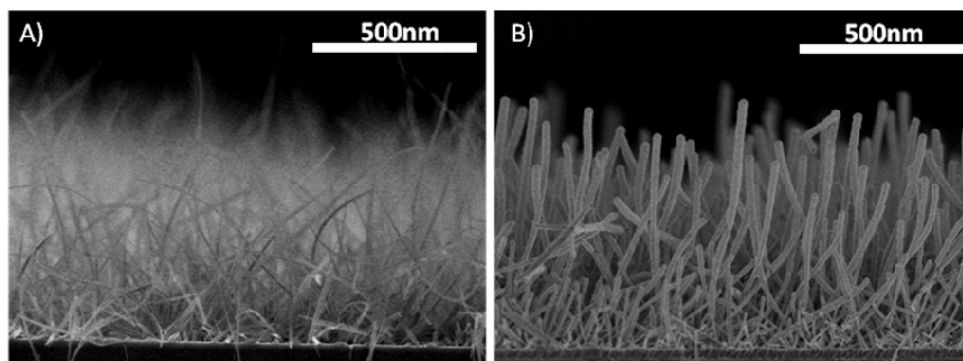


**Figure 1** – SEM images of: A) Single crystal organic nanowires made of made of Zinc Phthalocyanine; B) Conformal growth of the ZnO layer over the organic nanowires.

## References

- [1] A. Borrás, O. Groning, M. Aguirre, F. Gramm, P. Groning *Langmuir* **26** (2010), 5763.

## Flexible, Self-standing and Selective UV-VIS-NIR Optical Filters Based on Polymer Infiltration of Porous One Dimensional Photonic Crystals

Mauricio E. Calvo, J. R. Castro-Smirnov and Hernán Míguez

*Instituto de Ciencia de Materiales de Sevilla, Seville, Spain.*

\*contact e-mail: [Mauricio.calvo@icmse.csic.es](mailto:Mauricio.calvo@icmse.csic.es)

**Keywords:** flexible, photonic crystals, hybrid materials, Bragg mirrors

### Abstract

Herein we present a novel synthetic route to attain flexible and self standing optical filters with capability of selectively blocking radiation in the ultraviolet (UV), visible (Vis) and near infrared (NIR) regions. Shielding was achieved alternating metal oxide nanoparticle layers with different refractive index to obtain a porous one dimensional photonic crystal (1DPC). The mechanical properties of the ensemble are then enhanced by polymer (PDMS or polycarbonate) infiltration of those porous structures. [1] The method proposed yields uniform filling of the nanopores in the multilayer by the polymer, which allows lifting off the hybrid structure.[2] The final material combines the optical properties of the embedded nanoparticle multilayer and the mechanical properties of the polymer. Experimental evidence of the use of these materials as low-weight mirrors and as highly efficient UV protective films are also provided.[3]

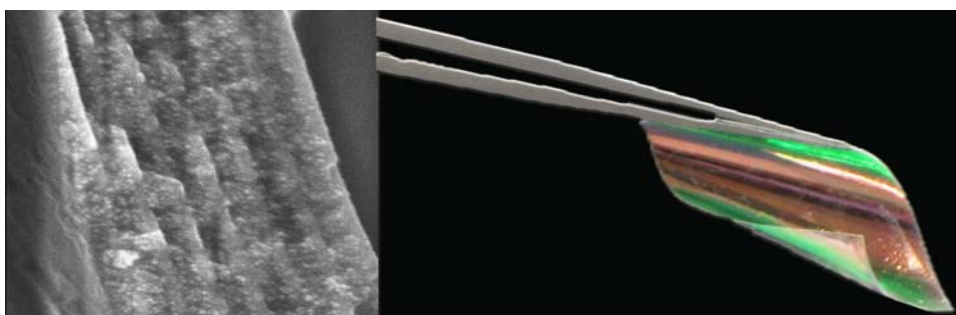


**Figure 1** – Cross Section FESEM image and optical image of a flexible hybrid one dimensional photonic crystals

### References

[1] O. Sánchez-Sobrado, M.E. Calvo, H. Míguez, *J. Mater. Chem* (Cover Story) (2010), **20**, 8240-8246

- [2] M.E. Calvo, J.R. Smirnov, H. Míguez *J. Polymer Sci. Part B* (2012) DOI:  
10.1002/polb.23087
- [3] M.E. Calvo, H. Míguez *Chem. Mater.* (2010), **22**, 3909-3915

## Photonic Crystals for Enhanced Light Harvesting in Dye Solar Cells

Carmen López-López,\* Silvia Colodrero, and Hernán Míguez.

*Instituto de Ciencia de Materiales de Sevilla, Consejo Superior de Investigaciones Científicas-Universidad de Sevilla, Américo Vespucio 49, 41092, Sevilla, Spain.*

\*contact e-mail: Carmen@icmse.csic.es

**Keywords:** dye sensitized solar cell; optical absorption amplification; porous one dimensional photonic crystals

### Abstract

Dye sensitized solar cells (DSSC) are photovoltaic devices based on the absorption of the sunlight by dye molecules to generate electricity. In order to improve the absorptance of the dye, the optical design of the cell can be modified by coupling nanoparticle 1D photonic crystal (1DPC)<sup>1</sup>. This 1DPCs are built by the deposition of SiO<sub>2</sub> and TiO<sub>2</sub> nanoparticles.<sup>2</sup> This mirror is able to efficiently localize incident light within the sensitized electrode in a targeted wavelength range. Furthermore, its porous mesostructure allows the diffusion of the electrolyte through the layers. New methods for increasing the porosity and the pore size of these nanoparticle films in a controlled way, while preserving the optical quality, will be presented.<sup>3</sup> In this way, the mass transport through the crystal is improved, as confirmed by impedance measurements.

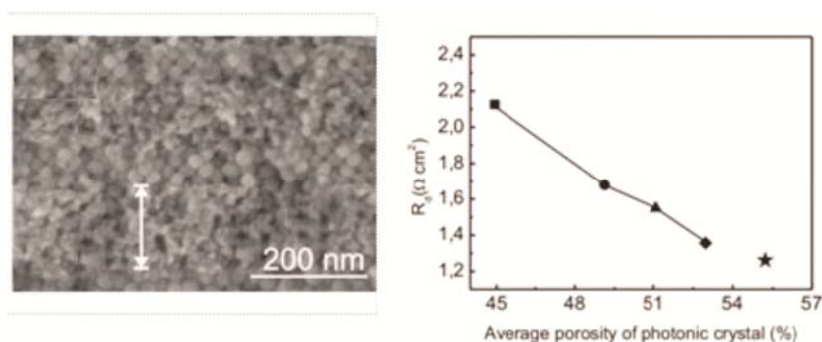


**Figure 1** – On right: FESEM image of a cross section of highly 1DPC showing the result of mixing a porogen with the nanoparticle suspensions and the annealing. On left: Diffusion resistance obtained at  $j=0$  mA versus average porosity of the 1DPC prepared using different porogen:np-TiO<sub>2</sub> weight ratios, namely, 0 (square), 0.25 (circle), 0.5 (triangle), 0.75 (rhombus). Data for the multilayer prepared using both porogen:np-TiO<sub>2</sub> and porogen:np-SiO<sub>2</sub> weight ratios of 0.5 are also shown (star).

## References

- (1) S. Colodrero, A. Mihi, L. Häggman, M. Ocaña, G. Boschloo, A. Hagfeldt, H. Míguez, *Adv. Mater.*, 2009, **21**, 764.
- (2) S. Colodrero, A. Mihi, J.A. Anta, M. Ocaña, H. Míguez, *J. Phys. Chem. C*, 2009, **113**, 1150.
- (3) C. López-López, S. Colodrero, S.R. Raga, H. Lindström, F. Fabregat-Santiago, J. Bisquert, and H. Míguez.

## Modification of Mesoporous Films by Electrochemical Doping: Impact on Photocatalytic and Photovoltaic Performance

Jesús Idígoras, Thomas Berger\* and Juan A. Anta\*

*Departamento de Sistemas Físicos, Químicos y Naturales, Área de Química Física,  
Universidad Pablo de Olavide, Crta. Utrera, km 1, E-41013, Spain.*

\*Corresponding authors: Tel.: +34 95434 9313; Fax: +34 95434 9814; E-mail:  
[tberger@upo.es](mailto:tberger@upo.es), [jaantmon@upo.es](mailto:jaantmon@upo.es)

**Keywords:** Electrochemical doping, nanostructured TiO<sub>2</sub> electrodes, photocatalysis, dye-sensitized solar cells.

### Abstract

The effect of reductive electrochemical doping of nanostructured TiO<sub>2</sub> electrodes on their photocatalytic and photovoltaic performance in dye-sensitized solar cells is studied. It is observed that accumulation of negative charge (compensated by proton insertion from supporting electrolyte) leads to an improvement of the photocurrent of water photooxidation<sup>1</sup> along with an improvement in the photoconversion efficiency of the doped electrodes with respect to the unmodified ones. The effect has been analyzed using small-perturbation electrochemical techniques<sup>2</sup> (impedance spectroscopy, intensity modulated photovoltage and photocurrent spectroscopies). The results showed that the better photocatalytic and photovoltaic efficiency is due to a more rapid electron transport combined with reduced recombination. The observed effect is analogous to that reported previously using light-soaking and cation intercalation treatments<sup>3,4</sup>.

### References

- [1] Berger, T.; Lana-Villarreal, T.; Monllor-Satoca, D.; Gomez, R. *Electrochemistry Communications* **2006**, *8*, 1713–1718.
- [2] Guillén, E.; Peter, L. M.; Anta, J. A. *J. Phys. Chem. C* **2011**, *115*, 22622–22632
- [3] Meekins, B. H.; Kamat, P. V. *ACS Nano* **2009**, *3*, 3437–3446.
- [4] Wang, Q.; Zhang, Z.; Zakeeruddin, S. M.; Gratzel, M. *J. Phys. Chem. C* **2008**, *112*, 7084–7092.





## **Session 3**

# **Multifunctional Nanoparticles and Nanostructures**



## Nanotechnology for life science: an example of bottom up approach, from PVD reactor to in-vivo evaluation

S. Lucas\*

*NARILIS – NAMur Research Institute for Life Sciences,  
Research center in Physics of Matter and Radiation (PMR), Laboratoire d'Analyses par Réactions Nucléaires (LARN), FUNDP University of Namur, Belgium*

\*contact e-mail: stephane.lucas@fundp.ac.be

### Abstract

In medicine, development of hybrid nanoparticles that can target vascular, extra-cellular or cell surface receptors is often considered as an attractive solution for cancer detection and treatment.

Here, we propose a new method to produce small and biocompatible gold nanoparticles (AuNPs) that specifically target the epidermal growth factor receptor (EGFR), a membrane protein overexpressed in several kinds of solid tumors.

In a first step, nanosized (2-10 nm) AuNPs are synthesized by plasma vapor deposition (PVD). The surface of these AuNPs is then functionalized in-situ in the plasma reactor by a coating of PPAA (plasma-deposited polyallylamine) before their transfer into solution. The PPAA coating enhances the stability of the AuNPs in an aqueous environment and allows the coupling with antibodies. Results about the investigation of unfunctionalized and functionalized nanosized nanoparticles by TEM, XPS and CPS Disc Centrifuge will be presented.

Second, EGFR was targeted by covalently coupled to Cetuximab antibodies (mAb) to the amino groups present in the polymeric shell of PPAA-coated AuNPs. Results about size, morphology, composition and dispersion of free and conjugated PPAA-coated AuNPs in solution, analyzed by Transmission Electron Microscope (TEM), CPS Disc Centrifuge, UV and Atomic Absorption analyses will be presented.

Third, in-vivo studies were performed by antibody firstly labeled with radioactive isotopes like  $^{125}\text{I}$  or  $^{89}\text{Zr}$  before being coupled to the PPAA-coated AuNPs and then injected in murine models xenografted with human cancer cells. Micro-PET studies showed that tumor uptake is not significantly different between free and nanoconjugated Cetuximab, highlighting the fact that the whole assembly (NP-PPAA-mAb) retains its recognition properties also in-vivo. SIMS analysis also demonstrated that Au is effectively present in the targeted organs.

Acknowledgments: the Targan project is a Waleo 2 project from the Walloon Region, Belgium. D. Bonifazi, V. Bouchat, O. Feron, L. Karmani, R. Marega, B. Masereel, N. Moreau, V. Valembois, T. Vander Borcht, C. Michiels and B. Gallez are partners of this project.



## TEM of hybrid Au nanoparticles capped with allylamine

Lionel Cervera Gontard<sup>a\*</sup>, Vanessa Valembois<sup>b</sup>, Asunción Fernández<sup>a</sup>, Takeshi Kasama<sup>c</sup>, Rafal Dunin-Borkowski<sup>d</sup>, Stéphane Lucas<sup>b</sup>

<sup>a</sup> *Instituto de Ciencia de Materiales de Sevilla (CSIC, 41092, Sevilla, Spain*

<sup>b</sup> *NARILIS – NAmur Research Institute for Life Sciences, Research center in Physics of Matter and Radiation (PMR), Laboratoire d'Analyses par Réactions Nucléaires (LARN), FUNDP University of Namur, Belgium*

<sup>c</sup> *Center for Electron Nanoscopy (CEN), Technical University of Denmark, DK-2800, Kongens Lyngby, Denmark*

<sup>d</sup> *Ernst Ruska-Centre for Microscopy and Spectroscopy with Electrons (ER-C) and Peter Grünberg Institute (PGI), Forschungszentrum Jülich, D-52425 Jülich, Germany*

\*contact e-mail: lionel.gontard@icmse.csic.es

**Keywords:** Gold, poly-allylamine, hybrid nanoparticles, TEM, EFTEM

### Abstract

Hybrid organic/inorganic nanoparticles (NPs) that are capped with polymers and naturally occurring biomolecules are of great interest in nanomedicine for targeting vascular, extra-cellular or cell surface receptors. Although the inorganic components of hybrid nanoparticles can be readily characterized by conventional electron microscopy techniques, the structural arrangement of the organic molecular components remains largely unknown [1]. This difficulty arises because soft materials intrinsically exhibit low electron-optical image contrast and are very sensitive to the ionizing radiation that is used in a conventional electron microscope, which results in both chemical and structural changes during measurements.

Here, we apply high-resolution transmission electron microscopy (TEM) and energy-filtered TEM to characterise Au NPs that are coated with polymerised poly-allylamine (PPAA), an organic compound with the formula  $C_3H_5NH_2$ . The PPAA coating enhances the stability of the AuNPs in an aqueous environment and allows their functionalization with, for example, antibodies [2]. The sample was synthesized using a novel method based on the stacking of alternating layers of PPAA, Au NPs, PPAA and NaCl formed by plasma vapor deposition (PVD), followed by dilution in water [3]. For TEM observation, a drop of the solution was deposited onto a C support on a Cu grid and dried in air. The supporting carbon films used for the experiments had thicknesses of below 10 nm and comprised either graphene flakes (Fig. 1a) or a layer of ultra-thin amorphous C (Fig. 1c).

The results shown in Fig. 1 illustrate that the polymeric PPAA coating of the Au NPs can be imaged in the TEM with sufficient contrast at an accelerating voltage of 300 kV at ambient temperature. Interestingly, the shape of the coating on the NPs remained stable even after some minutes of observation in the TEM, although the atomic structure of the organic material was then likely to have changed as a result of electron irradiation (beam damage). For most of the Au NPs, the capping layer is not uniform in

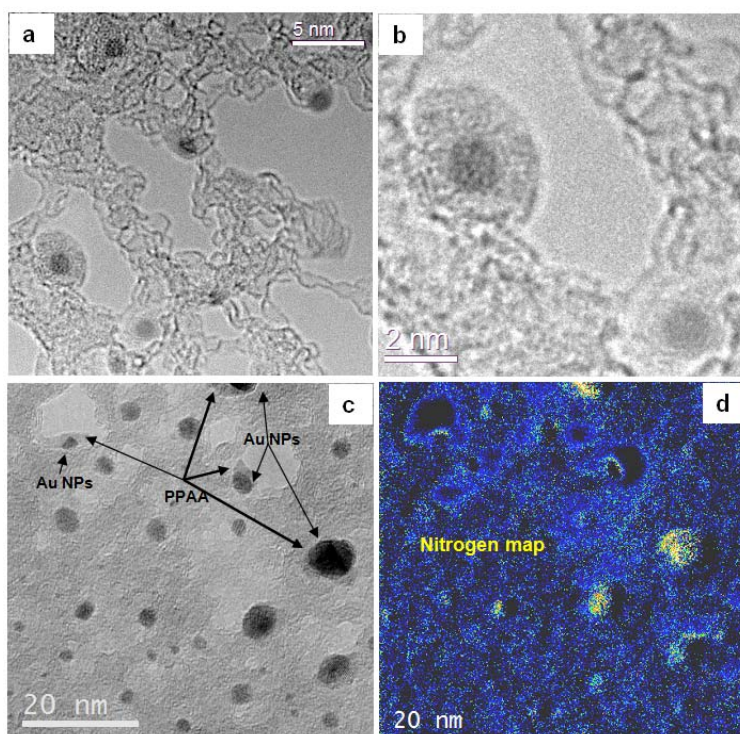


**Figure 1** – (a) High-resolution TEM image of Au NPs coated with PPAA deposited on graphene flakes. (b) Au nanoparticles with an organic capping layer that has a thickness of 1 nm. (c) TEM image of Au NPs deposited on ultrathin carbon. Most of the particles are covered with a non-uniform organic layer. (d) Map of nitrogen acquired from the region shown in (c) using EFTEM. The yellow color in the image is suggestive of the presence of N in PPAA associated with the capping of the NPs.

thickness. To confirm that the organic material at the surface of the NPs is PPAA, we used EFTEM to measure the presence and distribution of N, which is a constituent of the allylamine (Fig. 1d). Although specimen drift and/ or specimen damage has affected parts of the background subtracted elemental map shown in Fig. 1d, the result is suggestive of the presence of N associated with the positions of the Au particles.

In conclusion, by using the thinnest C supports in combination with EFTEM, it is possible to image and characterise hybrid Au NPs capped with PPAA.

In the future, image resolution and sensitivity will be improved by using lower beam accelerating voltages, lower specimen temperatures and low-dose imaging techniques to minimize electron beam

induced damage of the organic layers, in combination with the use of through-focal series restoration and spherical and chromatic aberration correction to maximize both visibility and spatial resolution in structural and chemical images.

## References

- [1] Richman E K & Hutchison J E, *ACS Nano* **3** (2009) 2441.
- [2] Masereel B et al., *Journal of Nanoparticle Research* **13** (2011) 1573.
- [3] Moreau N et al., *Plasma processes and polymers* **6** (2009) 5.

## Nanosecond-laser control of the dichroism in supported silver nanoparticles deposited by evaporation at glancing angles

A. N. Filippin<sup>1</sup>, Ana Borrás<sup>\*1</sup> and Agustín R. González-Elipe<sup>1</sup>

<sup>1</sup> Instituto de Ciencia de Materiales de Sevilla (ICMS, CSIC-US), Nanotechnology on Surfaces Lab., C/ Américo Vespucio 49, 41092, Sevilla, Spain.

\*contact e-mail: [anaisabel.borras@icmse.csic.es](mailto:anaisabel.borras@icmse.csic.es); [alejandro.filippin@icmse.csic.es](mailto:alejandro.filippin@icmse.csic.es);

**Keywords:** Silver nanoparticles, Surface Plasmon Resonance, Dichroism, Laser treatment

### Abstract

Silver nanoparticles (NP) depicting a well-defined Surface Plasmon Resonance (SPR) absorption were deposited on fused silica and silicon substrates by physical vapor deposition in a glancing angle (GLAD) configuration. The particles were characterized by Scanning electron Microscopy (SEM) and Atomic Force Microscopy (AFM) and their optical properties examined by UV-vis absorption spectroscopy using linearly polarized light. The effects of the deposition angle and sample thickness on the optical properties are thoroughly examined. It is found that the NPs present a certain anisotropy in shape and a significant optical dichroism produced by a different SPR absorption when using polarized light at 0° and 90°. Further control on the SPR wavelength and dichroism is achieved by irradiation of these materials with a nanosecond infrared Nd-YAG laser at different powers. Low power treatment produces an enhanced dichroism that is attributed to the preferential aggregation of the smallest metal particles at the longest dimension of the initially deposited anisotropic NPs. At higher powers, the dichroism is lost as a result of the reshape of the silver NP in the form of big spheres.

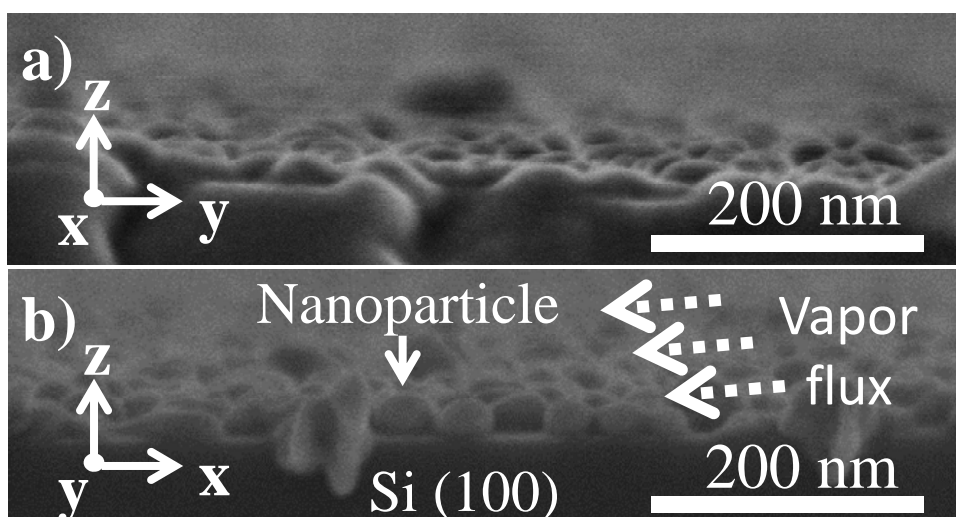


**Figure 1** – Cross section SEM micrographs of silver nanoparticles grown over Si (100). (a) View in the direction of the incoming silver flux. (b) Perpendicular to the gas flux.

## References

- [1] L. González.García, I. González-Valls, M. Lira-Cantu, A. Barranco, A. R. González.Elipe, *Energy & Environmental Science*, **4** (2011), 3426-3435.
- [2] J. D. Driskell, S. Shanmukh, Y. Liu, S. B. Chaney, X. J. Tang, Y. P. Zhao, R. A. Dluhy, *Journal of Physical Chemistry C*, **112** (2008), 895-901.
- [3] J. R. Sánchez-Valencia, J. Tourdet, A. Borrás, A. Barranco, R. Lahoz, G. F. de la Fuente, F. Frutos, A. R. González-Elipe, *Advanced Materials*, **23**, **7** (2011), 848-853.



**Session 4**  
**Catalytic Materials**



## Microstructure, chemical stability and conductivity of LSM based cathodes obtained by mechanochemical method at room temperature

R. Moriche<sup>a</sup>, M.J. Sayagués<sup>a</sup>, J.M. Córdoba<sup>a</sup>, D. Marrero<sup>b</sup> and F.J. Gotor<sup>a</sup>

<sup>a</sup> *Instituto de Ciencia de Materiales de Sevilla, Centro mixto CSIC-US, Av. Américo Vespucio 49, 41092 Seville, Spain.*

<sup>b</sup> *Dpto. Física Aplicada I, Facultad de Ciencias, Universidad de Málaga. Campus Teatinos s/n, 29071 – Málaga, Spain.*

\*contact e-mail: rocio.moriche@icmse.csic.es

**Keywords:** SOFC, cathode, mechanochemistry

### Abstract

Solid Oxide Fuel Cells (SOFCs) are thought to be a potential energy generation system because of their long-term stability, high efficiency and low pollution [1, 2]. Another important reason is that they are cheaper than another kind of fuel cells due to the fact that their components are ceramics [3].

The synthesis of ceramic components for these SOFCs have been widely studied by different methods but there are only a few papers published about obtaining them by mechanochemistry [4].

Cathodes based on solid solution of lanthanum strontium manganites with formula  $\text{La}_{1-x}\text{Sr}_x\text{MnO}_{3-\delta}$  (LSM) constitute a promising component for SOFCs and their behaviour depends strongly on the La/Sr ratio and their microstructure.

In the present work the LSM system ( $x=0.00, 0.25, 0.50, 0.75, 1.00$ ) have been synthesized by mechanochemical methods obtaining monophasic powders with a perovskite structure. The process was carried out using a high energy planetary ball milling equipment in air atmosphere at room temperature. The as-prepared samples were uniaxially pressed and heated at 1300 °C for 24 h getting a better crystallization to allow the microstructural analysis and the conductivity measurement. The chemical stability of LSM system with the most common anode (YSZ) has been studied by heating a mixture 50:50 wt% of them at 800, 900, 1000, 1100, 1200 and 1300 °C for 24 h. The nanostructured powders were characterized before and after heating by X-ray, electron diffraction, TEM and EDX analysis. The X-ray analysis shows the evolution of the solid solution structure as the Sr content increases. In this way, samples with  $x=0.00, 0.25, 0.50$  and  $0.75$  present a pseudo-cubic (p) and rhombohedral (r, R-3c) structures for pre-sintered and sintered samples, respectively. While phase with  $x=1$  presents hexagonal symmetry (h, P63/mmc) after sintering.

The as-prepared samples exhibit nanocrystalline character (10-20 nm). After temperature treatment the crystallites size increases though it remains quite small (200-300 nm) for their application as cathode. Figure 1a shows a HR image along [211]<sub>r</sub> for  $x=0.25$  sample after sintering. The interplanar spacing is marked with arrows.

Figure 1b presents the HRTEM of  $x=1.00$  phase through  $[010]_h$  where some stacking faults can be seen, marked in the figure as well as the interplanar distances.

Electrical conductivity was measured by the four-points method. As it is shown in Figure 2, up to  $x=0.50$  the higher the Sr content, the better the conductivity, probably due to a raise in the number of defects. The values reach  $100 - 400 \text{ Scm}^{-1}$  for the intermediated phases at temperatures of  $25 - 850 \text{ }^\circ\text{C}$ . It has to be pointed out that  $x=0.25$  phase shows a ferromagnetic to paramagnetic transition at  $71 \text{ }^\circ\text{C}$  which has to be considered for the working range of the cell because of its influence in the conductivity.

To summarize, nanostructured LSM powders can be obtained at room temperature by using mechanochemistry what causes a decrease in the cost of the cell fabrication showing a good chemical stability and conductivity.

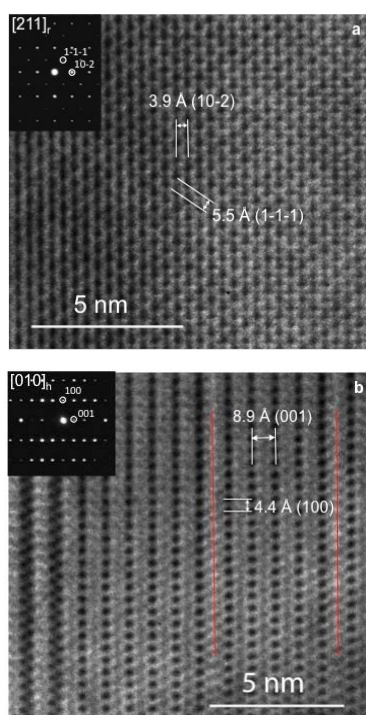


**Figure 1** – HRTEM images and the corresponding EDPs of (a)  $x=0.25$  and (b)  $x=1.00$ .

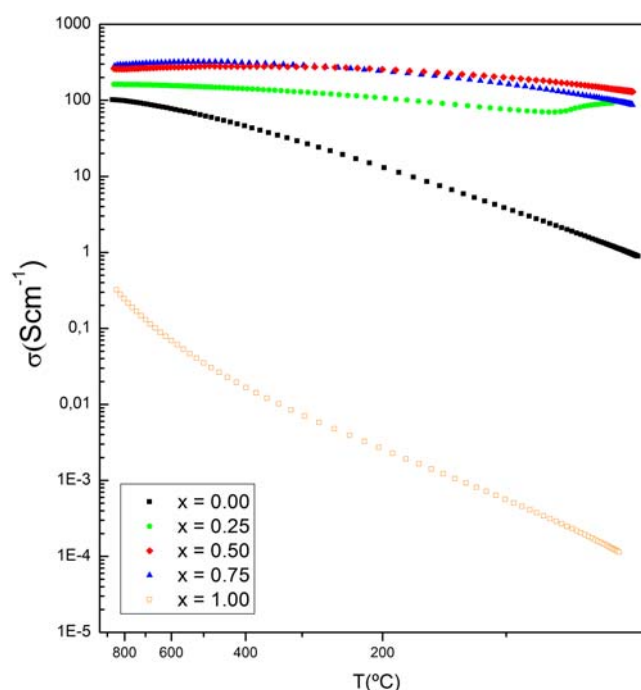


**Figure 2** – Electrical conductivity of the system  $\text{La}_{1-x}\text{Sr}_x\text{MnO}_{3-\delta}$  measured by four-points method.

## References

- [1] M. Wang, K.D. Woo and C.G. Lee, Energy Conversion and Management, **52** (2011), p. 1589.
- [2] X. Zhu, Z. Lü, B. Wei, X. Huang, Y. Zhang and W. Su, J. of Power Sources, **196** (2011), p. 729.
- [3] Y.J. Park, Kim and H. Kim, International J. of hydrogen Energy, **36** (2011), p. 9169.
- [4] M.J. Sayagués, J.M. Córdoba and F.J. Gotor, J. of Solid State Chem., **188** (2012), p. 11.

## Quantitative electron microscopy for rationalizing the activity and stability of nanocatalysts

JJ Delgado\*, E. del Río, M. López-Haro, X. Chen, J.M. Cies, JJ Calvino, S. Trasobares and S. Bernal

*Departamento de Ciencia de los Materiales e Ingeniería Metalúrgica y Química Inorgánica. Facultad de Ciencias. Universidad de Cádiz. Campus Rio San Pedro, Puerto Real, 11510-Cádiz, Spain*

\*contact e-mail: [juanjose.delgado@uca.es](mailto:juanjose.delgado@uca.es)

**Keywords:** STEM-HAADF, nanocatalyst, HREM, CO Adsorption, Catalytic activity

### Abstract

It is unquestionable that one of the most important challenges of our society is the development of new energy strategies to tackle global warming and exhaustion of fossil fuels. Therefore, the design of innovative low-cost and environmentally friendly energy storage and conversion systems is crucial for stable economic growth in a world whose energy needs are continuously increasing. In this context, catalysis has been proven as a critical enabling science for developing the use of alternative feedstocks, such as biomass or hydrogen, and increasing energy production efficiency [1].

Real catalysts commonly are complex multicomponent systems whose characterization usually demands an insight at the atomic level, and they are continuously posing new challenges and calling for further improvements in Electron Microscopy techniques. On the other hand, real catalysts contain morphological, structural and compositional heterogeneities and it is also obvious the need of developing new methodologies, based in statistical studies, that will give us a real picture of our catalyst. This point is really crucial for the rationalization of structure-activity-selectivity relationships and understanding the deactivation processes. This approach is very promising in order to bridge the gap between model surfaces and supported nanoparticles studies, which would greatly contribute to the real innovative design of new material with tailored properties.

The major goal of this contribution will be to review, using a number of examples from our most recent work, the possibilities of (Scanning) Transmission Electron Microscopy to reveal the ultimate details of the structure of these Oxide and Metal/Oxide systems and how this information allow us gaining some understanding of how they work as catalysts. The lecture will focus on understanding the interaction of CO with gold catalysts supported on ceria-based oxides. This is a relatively new family of materials which has received increasing attention because of its outstanding activity in a number of relevant catalytic reactions for energy production such as PROX and WGS, having in common the participation as reactant of the CO molecule [2].

High Resolution Transmission and High Angle Annular Dark Field-Scanning-Transmission Electron Microscopy (HRTEM and HAADF-STEM) are combined, in an appropriate manner, with FTIR spectroscopy and Volumetric CO Adsorption studies

and nano-structural computer modeling techniques. We have developed a methodology to obtain the contribution of the surface atoms with a certain coordination number to the total dispersion. This information, in combination with the quantitative CO adsorption on the metal data, allows identifying the coordination number of the gold surface sites where the CO is adsorbed [3]. The approach consists in the following steps: 1) Determination of the particle morphology for the supported Au nano-particles on the basis of HREM studies, modeling and image simulation (Figure 1 a-c). 2) Accurate determination of the gold particle size distribution performed this analysis by measuring a sufficiently high number of particles (above 250) on different STEM-HAADF micrographs. 3) Generation of a set of model gold nanoparticles covering the whole range of sizes observed in the experimental distribution (Figure 1 d-f). 4) Determination of the contribution of each coordination number.

Special attention will be paid to the discussion of the chemical information that can be obtained from the correlation of the CO adsorption on the metal and the support data with the nano-structural properties of the corresponding catalysts.

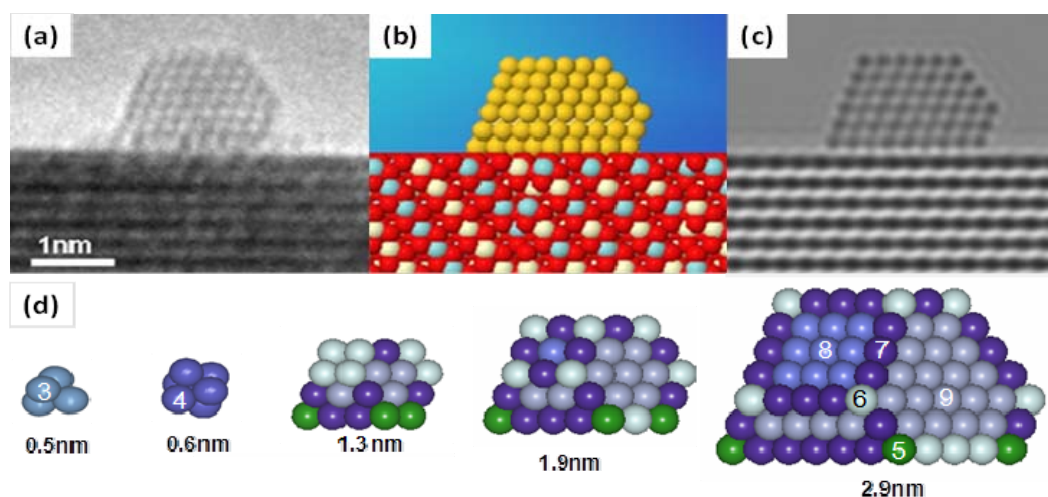


**Figure 1** – Representative HREM image of a gold nanoparticle supported on a Ce-ZrTb mixed oxide (a). The corresponding model (b) and image simulation (c) are also included. (d) Illustrates a series of gold nanoparticle models with different sizes, where the coordination numbers are marked.

## Acknowledgements

This work has received financial support from Spanish MICINN/FEDER-EU (Project MAT2008-00889-NAN) and EULANEST/MICINN (PIM2010EEU-00138).

## References

- [1] G.M. Whitesides and G.W. Crabtree, *Science*, **315** (2007), 796.
- [2] H. Daly, A. Goguet, C. Hardacre, F.C. Meunier, R. Pilasombat, D. Thompsett, *J. Catal.* **273** (2010), 257.
- [3] M. Lopez-Haro, J.J. Delgado, J.M. Cies, R.E. del, S. Bernal, R. Burch, M.A. Cauqui, S. Trasobares, J.A. Perez-Omil, P. Bayle-Guillemaud and J.J. Calvino, *Angew. Chem. Int. Ed.*, **49**(2010), 1981.

## The Co-Ru-B series as catalysts for hydrogen generation: synergistic effect, chemistry and nanostructure

G.M. Arzac<sup>1\*</sup>, T.C. Rojas<sup>1</sup>, L.C. Gontard<sup>1</sup>, A. B. Hungría<sup>2</sup>, L. E. Chinchilla<sup>2</sup> and A. Fernández<sup>1</sup>

1. Instituto de Ciencia de Materiales de Sevilla (ICMS), CSIC-Universidad de Sevilla.  
C/ Américo Vespucio 49. Isla de la Cartuja, 41092 Seville, Spain.

2. Departamento de Ciencia de Materiales, Ingeniería Metalúrgica y Química  
Inorgánica, Facultad de Ciencias, Universidad de Cádiz, 11510 Puerto Real, Cádiz,  
Spain.

\* contact e-mail: [gisela@icmse.csic.es](mailto:gisela@icmse.csic.es).

**Keywords:** hydrogen generation, sodium borohydride, Co-Ru-B catalysts, synergistic effect, nanoalloys.

### Abstract

Catalysed sodium borohydride ( $\text{NaBH}_4$ ) hydrolysis ( $\text{NaBH}_4 + 2\text{H}_2\text{O} \rightarrow 4\text{H}_2 + \text{NaBO}_2$ ) is a safe and controllable method to store and produce hydrogen for PEMFCs (Polymer Exchange Membrane Fuel Cells) for portable applications [1]. Within catalysts, Co-B based materials are the most used because they are much more cost-effective. It is well known that the addition of a second metal M' to form a Co-M'-B material produces an enhancement in catalytic activity. In particular, the Co-Ru-B system (with variable Ru content from 0 to 100 atomic percent of total metal) has been studied by us and nanostructure has proven to play a key role in the comprehension of the synergistic effect in catalytic activity [2,3].

Many questions about our Co-Ru-B system are still unsolved. Previous BF TEM (Bright Field Transmission Electron Microscopy) and SEM (Scanning Electron Microscopy) images suggested that catalysts may be porous and surrounded by a lightweight veil, especially for the samples with lower Ru content [3]. Due to the complexity of the Co-Ru-B-(O) system XPS (X-Ray Photoelectron Spectroscopy) and TEM/EELS (TEM/Electron Energy Loss Spectroscopy) analyses did not show clear evidence of the formation of a Co-Ru nanoalloy or intermix [2]. On the other hand the exact particle size was not studied.

In this work five catalysts from the Co-Ru-B series with variable Ru content (expressed as Ru atomic percent of total metal) were prepared by chemical reduction [2]. STEM/HAADF (Scanning TEM /High Angle Annular Dark Field) images, as well as electron tomography have confirmed that catalysts are porous and covered in part with a lightweight veil. The higher the Ru content, the thinner the veil. DF TEM (Dark Field TEM), together with HRTEM (High-Resolution TEM) has shown that the 13% Ru Co-Ru-B catalyst is composed of small crystalline cores of ~0.2 nm diameter (Figs. 1a and 1b) in contrast to previous XRD (X-Ray Diffraction) measurements which indicated that the sample was amorphous [2]. For higher Ru content particles become bigger and more crystalline reaching a 2-8 nm particle size for the 100% Ru (Ru-B) sample (Fig.1c). EDX and EELS mapping with high lateral resolution have shown that Co and Ru appear separated suggesting that there is no formation of a Co-Ru nanoalloy. This result may be in accordance to Co segregation effect found through previous XPS

quantitative measurements [3]. Both metals appear to be intermixed forming either single  $\text{Co}^0$  and  $\text{Ru}^0$  or Co-B-O and Ru-B-O phases. These findings support our previously idea that the breaking in catalytic activity for the Ru-B material is due to the formation of higher metallic cores (so called by us “nanostructural transition”) [2].

The results presented here contribute to fully understand the synergistic effect in catalytic activity for the Co-Ru-B series. This effect is attributed to the conservation of the microstructure previously observed in a pure Co-B material for the Co-Ru-B series (except for the Ru-B sample) which maintains a high degree of dispersion of the active metals [2,3].

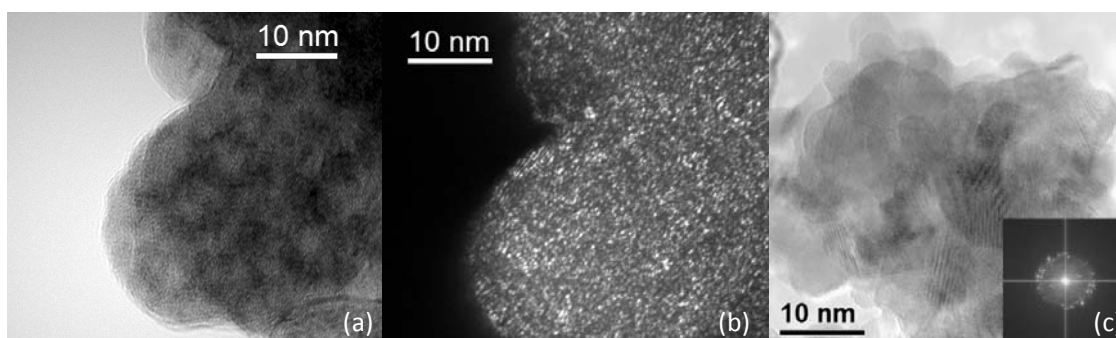


**Figure 1.** (a) BF and (b) DF TEM micrographs of the same area of the 13% Ru (atomic percent of total metal) Co-Ru-B catalyst. The speckle contrast arises from the diffraction of very small crystallites with sizes below 0.5 nm. (c) HRTEM micrograph of the 100 % Ru (atomic percent of total metal) Ru-B catalyst and the corresponding diffractogram (inset). The sample is formed by large crystals with sizes between 2-8 nm.

## References

- [1] B.H. Liu, Z.P. Li, *J. Power Sources*, **187** (2009), 527-534.
- [2] G.M. Arzac, T.C. Rojas, A. Fernández, *Appl. Catal. B: Environ.* (2012) <http://dx.doi.org/10.1016/j.apcatb.2012.02.013>.
- [3] G.M. Arzac, T.C. Rojas, A. Fernández, *Chem. Cat. Chem.*, **3** (2011), 1305-1313.



## Looking into Copper in CO-PROX Catalysts: A Multitechnique Approach

Guillermo Munuera

*Departamento de Química Inorgánica, Universidad Sevilla and Instituto de Ciencia de Materiales de Sevilla (Centro Mixto US-CSIC), Spain*

contact e-mail: [munuera@us.es](mailto:munuera@us.es)

**Keywords:** Copper oxide; Ceria-based catalysts; CO-PROX; XPS/XAES; DRIFTS

### Abstract

Production of H<sub>2</sub> for proton exchange membranes fuel cells (PEMFC) is usually accomplished by a multy-step process including reforming of hydrocarbons followed by water gas-shift (WGS) and a final preferential (or selective) oxidation of CO in the H<sub>2</sub>-rich stream resulting from such processes (CO-PROX), which is one of the most straightforward method to achieve acceptable CO concentrations (below ca. 100 ppm) compatible with an efficient handling of the fuel by the Pt alloy anode usually employed in the PEMFC.

A family of CO-PROX catalysts is emerging in the literature, constituted by closely interacting copper oxide and ceria, with excellent properties in terms of activity, selectivity and resistance to CO<sub>2</sub> and H<sub>2</sub>O, what could make them strongly competitive particularly owing to their lower cost (in comparison to usual catalysts based on supported platinum).

Although reaction models for CO oxidation (competing or not with H<sub>2</sub> oxidation, as it occurs under CO-PROX conditions) have been proposed for these type of catalysts on the basis of indirect analysis of redox or catalytic properties, only direct evidence of the redox changes taking place in the catalysts under CO-PROX conditions has been recently reported [1].

Combining different techniques (e.g. HRTEM, XRD STEM-XEDS, DRIFTS, XAFS, XPS/XAES, LEIS, etc.) to characterize the *as prepared* catalysts and/or under operando conditions, the results stress that the particular ability of copper-ceria catalysts for the CO-PROX, and related processes, could be essentially attributed to the synergistic redox properties exhibited upon formation of copper oxide-ceria interfacial sites which promotion strongly depends on their dispersion degree and/or related degree of interaction with ceria. The present contribution revises these studies and analyses issues related to the direct catalytic/redox correlations at the interface of copper oxide and ceria in this type of catalysts.

### References

[1] Gamarra, D.; Munuera, G.; Hungria, A.B.; Fernandez-Garcia, M.; Conesa J.C.; Midgley, P.A.; Wang, X.Q.; Hanson, J.C.; Rodriguez, J.A.; Martinez-Arias, A. *J. Phys Chem C* **2007**, 111, 11026-11038 *and other references therein of these authors*



## Posters



## **Session 1**

### **New trends in advanced nanoscopies**



## Comparative oxidation resistance of CrAlN, CrAlYN and CrAlZrN films by electron microscopies and EELS techniques

T.C. Rojas<sup>a</sup>, S. Domínguez-Meister<sup>a\*</sup>, S. El Mrabet<sup>a</sup>, M. Brizuela<sup>b</sup>, A. García-Luis<sup>b</sup>, J.C. Sánchez-López<sup>a</sup>

<sup>a</sup>*Instituto de Ciencia de Materiales de Sevilla (CSIC-Univ. Sevilla), Avda. Américo Vespucio 49, 41092-Sevilla, Spain.*

<sup>b</sup>*TECNALIA, Mikeletegui Pasealekua, 2 20009 Donostia-San Sebastián, Spain.*

\*s.dominguez@csic.es

**Keywords:** CrAlN, Thin film, Magnetron Sputtering, Electron Microscopy, EELS Spectroscopy, Oxidation Resistance.

Magnetron sputtered chromium aluminium nitride films are excellent candidates for advanced machining and protection for high temperature applications. In this work CrAlN-based coatings including Y or Zr as dopants are deposited by d.c. reactive magnetron sputtering on silicon substrates using metallic targets and Ar/N<sub>2</sub> mixtures. The influence of the incorporation of Y and Zr as dopants (content  $\approx$  2 at. %) in terms of oxidation resistance is studied by means of X-ray diffraction (XRD), cross-sectional scanning electron microscopy (X-SEM) and energy dispersive X-ray analysis (EDAX). The chemical bonding and microstructure are investigated using a transmission electron microscope (TEM), electron diffraction (ED) and electron energy-loss spectroscopy (EELS). The hardness properties are found in the range of 30-32 GPa with H/E ratios close to 0.1. The improvement in oxidation resistance after heating in air at 1000°C as compared to pure CrN coating is manifested in the formation of an outer layer rich in (Al,Cr)<sub>2</sub>O<sub>3</sub> that protects the underneath coating from oxygen diffusion. The best performance obtained with the CrAlYN film is investigated by in situ annealing of this sample inside the TEM in order to gain knowledge about the structural and chemical transformations induced during heating.





## Characterization of iron (III) oxide nanorods by Atomic Force Microscopy (AFM), Scanning Electronic Microscopy (SEM) and Transmission Electronic Microscopy (TEM).

M.V. de Paz <sup>a</sup>, C. Cerrillos <sup>\*b</sup> and F. Varela <sup>b</sup>

<sup>a</sup> *Departamento de Química Orgánica y Farmacéutica, Facultad de Farmacia, Universidad de Sevilla, c/ Profesor García González nº 2, Spain.*

<sup>b</sup> *Centro de Investigación, Tecnología e Innovación de la Universidad de Sevilla, Avda. Reina Mercedes 4-b, 41012 Sevilla, Spain.*

\*contact e-mail: ccerrillos@us.es

**Keywords:** Field emission SEM, TEM, AFM and Nanorods.

### Abstract

Superparamagnetic iron oxide particles are nanoparticles currently used for biomedical applications: drug delivery systems, contrast agents in magnetic resonance imaging, etc. [1, 2]

Different physicochemical properties such as final size and size distribution are key factors in their use in the human body.

We had characterized iron (III) oxide nanorods by different techniques: AFM, Field emission SEM and TEM.

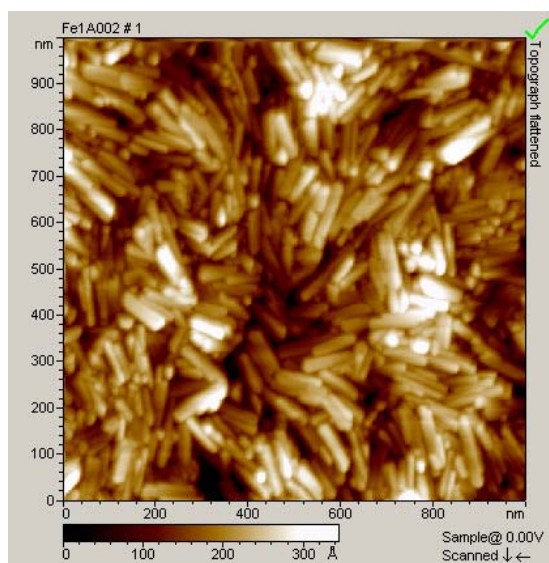


**Figure 1** – AFM images iron oxide nanorods on mica by Spin coating.

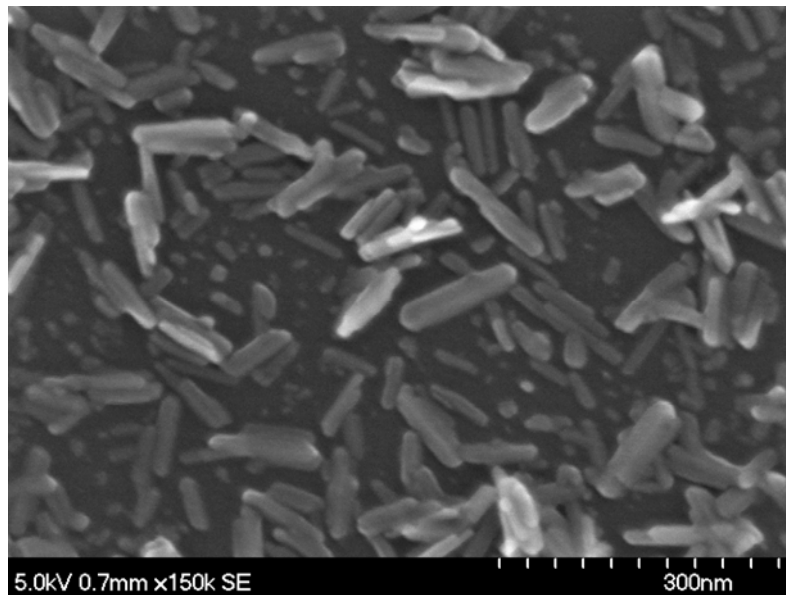


**Figure 2** – Field emission SEM images iron oxide nanorods on silicon by Spin coating.

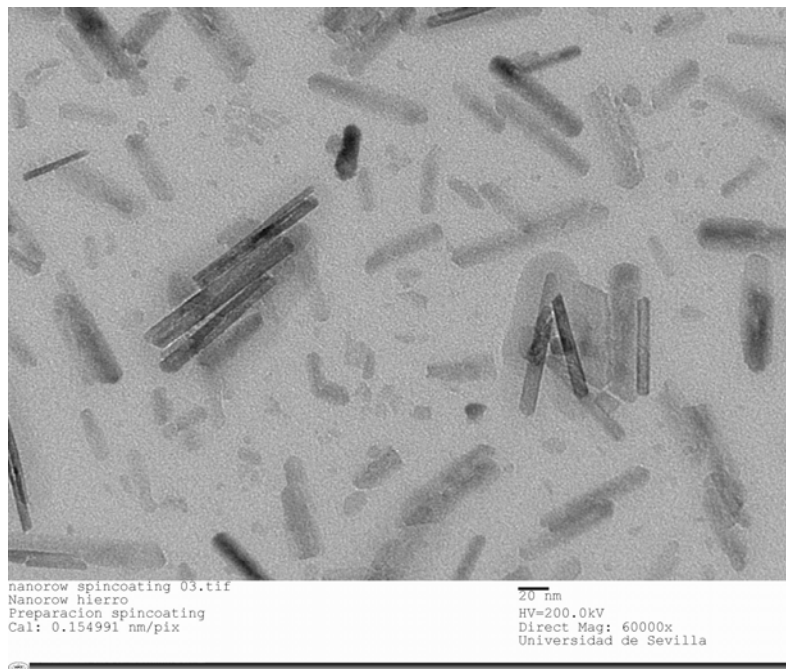


**Figure 3** – TEM images iron oxide nanorods by Spin coating.

## References

- [1] Arias, J. L.; López-Viota, M.; Ruiz, M. A. *Ars. Pharm.*, **49**(2), (2008), 101-111
- [2] Wu, L.; Cao, Y.; Liao, C. Huang, J.; Gao, F. *Eur. J. Radio.*, **80**(2) (2011), 582-589.

## Exposure of a filter feeding bivalve to gold nanoparticles: Location study by the STEM mode in a SEM-FEG microscope

C.A. García-Negrete<sup>1</sup>, M.C. Jimenez de Haro<sup>1</sup>, M. Volland<sup>2</sup>, M. Hampel<sup>2</sup>, J. Blasco<sup>2</sup>,  
A.Fernández<sup>1\*</sup>

<sup>1</sup> Instituto de Ciencia de Materiales de Sevilla, CSIC-Univ. Sevilla, Avda. Américo  
Vespucio 49, 41092-Sevilla, Spain.

<sup>2</sup> Instituto de Ciencias Marinas de Andalucía (ICMAN-CSIC), Campus Universitario  
Río San Pedro, 11519 Puerto Real, Spain.

\*contact e-mail: asuncion@icmse.csic.es

**Keywords:** Low energy STEM, STEM-in-SEM, ecotoxicity, gold nanoparticles, bivalve

### Abstract

Ecotoxicological risks in non target organisms associated with NPs are showing increasing consideration in the literature [1-3]. Thus in this study, the marine bivalve *Ruditapes philippinarum* was chosen as ecotoxicological model considering also its important filtering activity for nutritional and respiratory purposes. The STEM-in-SEM (scanning transmission electron microscopy in the scanning electron microscope) technique has been used in this paper to study the uptake of citrate stabilized gold nanoparticles (NPs), into digestive gland and gills tissues, upon exposure of the marine bivalve to Au NPs in seawater media.

The STEM-in-SEM offers contrast enhancement over TEM (transmission electron microscopy) due to lower electron energy in the SEM [4]. The increased electron scattering cross-section enables better insight into the morphology of low Z materials, such as polymers, often eliminating the need for heavy metal stain applications [1]. The localization of high Z nanoparticles in low Z tissue matrices is presented here by using the STEM-in-SEM coupled to EDX analysis as a powerful technique.

For “in vivo” experiments the organisms were exposed for 28 days in the laboratory to citrate reduced gold NPs (20 – 30 nm particle size) added to natural filtered seawater (concentrations of 6 and 30  $\mu\text{g}\cdot\text{L}^{-1}$  total gold). Samples (digestive gland and gills tissues) were taken throughout the exposure period in order to monitor the location and evolution of gold. For “in vitro” experiments dissected portions of digestive gland and gill tissues were immersed in Au NPs colloidal solutions at different concentrations in fresh and seawater media. Dissection, fixation, drying, embedding in resine, staining and ultramicrotome cutting were used for preparation of tissue slices. New results are presented in this paper in relation to Au location and distribution at the clam tissues. It is also worth to mention that thicknesses of 300 nm for the tissue slices gave optimal reproducible results. For thinner samples it is likely that the particles can be removed from the sample field of view by the cutting tool edge during preparation of slices.

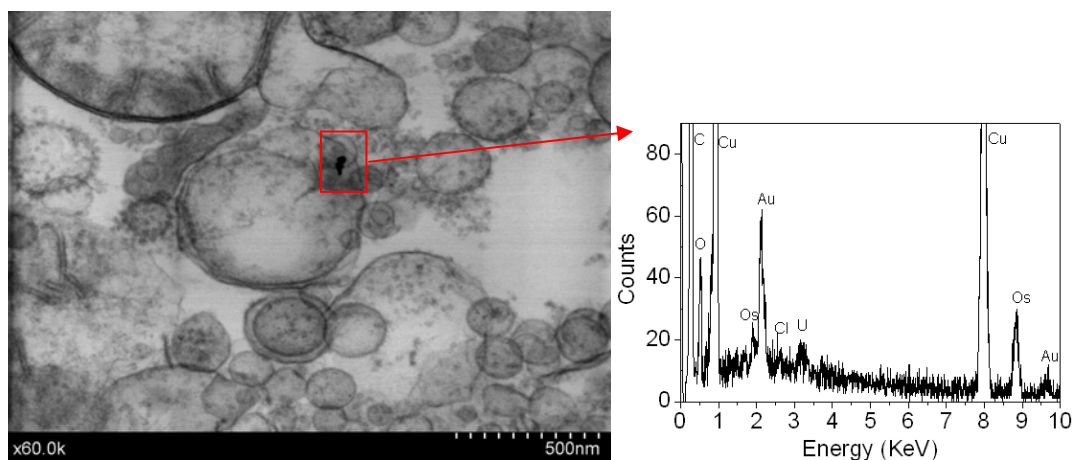


**Figure 1** – Left: SEM-FEG image (transmission mode) of a 300 nm slice of digestive gland tissue. Right: EDX spectrum from the area containing the Au NPs. Tissue sample obtained after 28 days “in vivo” exposure.

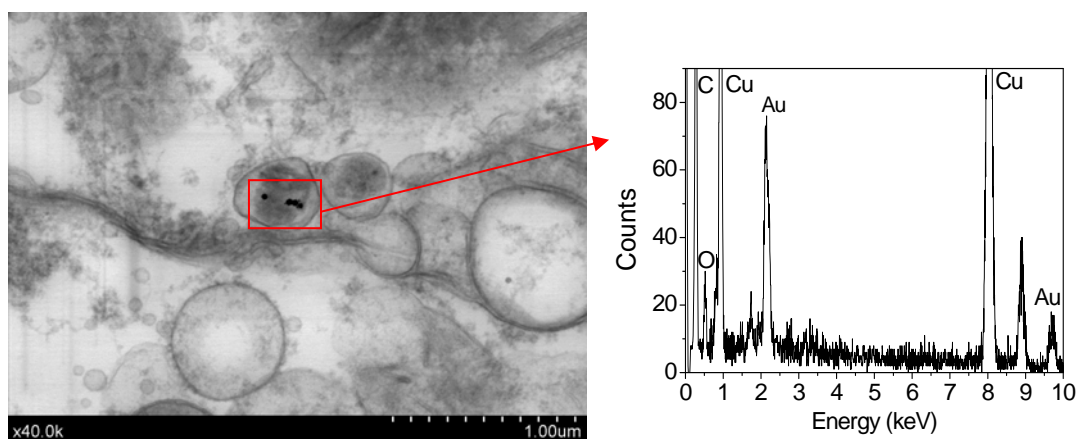


**Figure 2** – Left: SEM-FEG image (transmission mode) of a 300 nm slice of gills tissue. Right: EDX spectrum from the area containing the Au NPs. Tissue sample obtained after 2 hours “in vitro” exposure.

## References

- [1] A. Lapresta-Fernández, A. Fernández, J. Blasco, *Trends in Analytical Chemistry*, **32** (2012), 40.
- [2] A. Lapresta-Fernández, A. Fernández, J. Blasco. *Environment International*, **39** (2012), 148.
- [3] S. Tedesco, H. Doyle, J. Blasco, G. Redmond, D. Scheehan. *Comp. Biochem. Physiol.* **C151** (2010), 167
- [4] O.Guise, C. Strom, N. Preschilla. *Microsc Microanal*, **14**(Suppl2) (2008), 678.

## **Session 2**

### **Photonic and low dimensional nanostructures**



## Plasma assisted fabrication of wire-on-wire organic and hybrid 1D nanostructures

M. Alcaire<sup>\*1</sup>, Z. Saghi<sup>2</sup>, J. C. González<sup>1</sup>, A. Barranco<sup>1</sup>, A. R. González-Elipe<sup>1</sup> and A. Borrás<sup>1</sup>

<sup>1</sup> *1 Instituto de Ciencia de Materiales de Sevilla (ICMS, CSIC-US), Nanotechnology on Surfaces Lab., C/ Américo Vespucio 49, 41092, Sevilla, Spain.*

<sup>2</sup> *Department of Materials Science and Metallurgy University of Cambridge, Pembroke Street CB2 3QZ Cambridge, United Kingdom*

\*contact e-mail: maria.alcaire@icmse.csic.es

**Keywords:** organic nanowires, hybrid, hierarchical nanostructures, self assembly, soft plasma etching

### Abstract

In this communication we report on the fabrication of three different 1D organic heterostructures by the combination of two vacuum methodologies: physical vapor deposition and soft plasma etching. The field of small molecules organic 1D nanostructures has deserved an especial interest during the last years because the different applications of these nanostructured based on phthalocyanines, rubrene and perylenes in photonics, photovoltaic, photocatalysis, microelectronic and nanosensing applications. The controlled fabrication in high density of heterostructured organic nanowires has become a hot topic as consequence of their applications in the aforementioned fields as well as in the study of model systems for 1D n-p heterojunctions. Within this framework and taking as starting point the synthesis of single crystal organic nanowires (ONWs) by physical vapor deposition [1] on processable substrates we have explored the fabrication of wire-on-wire organic and hybrid junctions fabricated by combination of PVD for small molecules with oxygen plasma etching at controlled temperatures [2]. A thorough description of the different processes and advanced characterization of these novel materials are included.

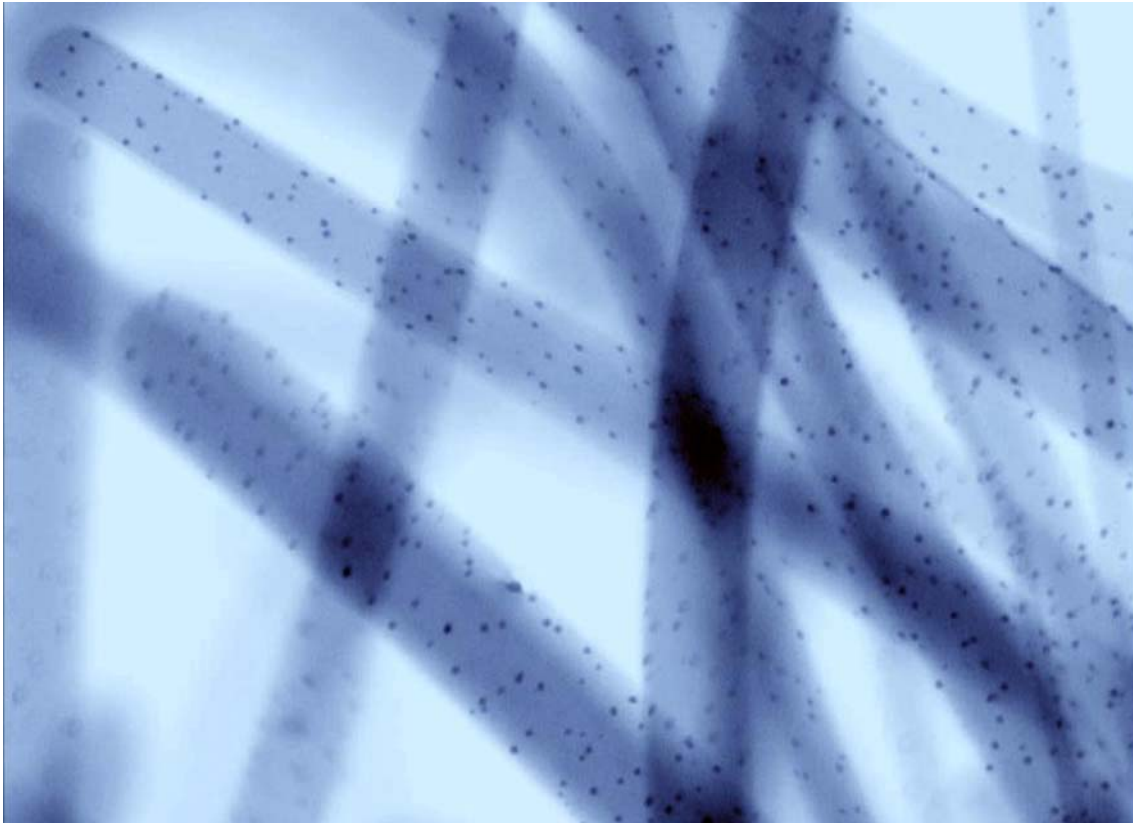


**Figure 1** – STEM micrograph of hybrid Co-NPs/CoPC-NWs formed by oxygen plasma treatment at room temperature of CoPC NWs.

### References

- [1] A. Borrás, M. Aguirre, C. Lopez-Cartes, O. Groening and P. Groening *Chem. Mater.* 2008, 20, 7371-7373.
- [2] M. Alcaire, J. R. Sanchez-Valencia, F. J. Aparicio, Z. Saghi, J. C. Gonzalez-Gonzalez, A. Barranco, Y. Oulad-Zian, A. R. Gonzalez-Elipe, P. Midgley, J. P. Espinos, P. Groening and A. Borrás *Nanoscale* 2011, 3, 4554-4559.



## Luminescent hybrid TiO<sub>2</sub> nanocomposite thin films prepared by glancing angle PVD for photonic sensing

Pedro Castellero<sup>a,b\*</sup>, Manuel Cano<sup>a</sup>, Javier Roales<sup>a</sup>, Juan R. Sánchez-Valencia<sup>b</sup>,  
Ángel Barranco<sup>b</sup>, Agustín R. González-Elipe<sup>b</sup> and José María Pedrosa<sup>a</sup>

<sup>a</sup> *Departamento de Sistemas Físicos, Químicos y Naturales, Universidad Pablo de Olavide, Carretera Utrera km 1, E-41013 Sevilla, Spain.*

<sup>b</sup> *Instituto de Ciencias Materiales de Sevilla, Universidad de Sevilla-CSIC, Américo Vespucio 49, E-41013 Sevilla, Spain.*

\*Corresponding author: pedro.castillero@icmse.csic.es

**Keywords:** TiO<sub>2</sub>, porphyrin, nanocomposite, dye, GLAD-PVD.

### Abstract

This work studies the fabrication of transparent TiO<sub>2</sub> columnar thin films for the fabrication of hybrid nanocomposite materials. The thin films have been prepared by glancing angle physical vapor deposition (GLAD-PVD). This technique permits the fabrication of oxide thin films with tailored porous columnar microstructures. The good optical properties of the TiO<sub>2</sub> thin films (transparency and controlled refractive index) and the well-defined porous structure obtained make these materials ideal candidates as hosts for the incorporation of functional guest molecules.

Two types of luminescent dyes have been incorporated the TiO<sub>2</sub> thin films from their corresponding solutions. The first one is a tetracationic porphyrin (TMPyP) that is infiltrated by simple immersion into solutions at controlled pHs. This molecule is incorporated in the porous films by electrostatic interaction. The second is a carboxy porphyrin (TCPyP) that is infiltrated in the porous thin films by immersion into solutions at controlled concentration values. In this case the molecule is chemically bind to the oxide surface.

These luminescent hybrid nanocomposite thin films are studied as active components of photonic sensing devices.

### References

- [1] P. Castellero et al., ACS Applied material and interfases, **2** (2010), 712-721.
- [2] M. Cano et al., Sensor and actuator B, **150** (2010), 764-769.
- [3] Y. Gaillard et al., Journal of Physics D: Applied Physics, **42**, (2009), 145305.
- [4] J. Rochford et al., J. Am. Chem. Soc., **129**,(2007), 4655-4665.



## Tailored luminescent emission of dyes embedded in porous resonators

A. Jiménez-Solano<sup>a\*</sup>, J. M. Luque<sup>a</sup>, M. E. Calvo<sup>a</sup>, ; F. Fernández-Lázaro<sup>b</sup>, ; H. Míguez<sup>a</sup>.

<sup>a</sup> Consejo Superior  
de Investigaciones Científicas (Spain)  
<sup>b</sup> Univ. Miguel Hernández de Elche (Spain)

\*contact e-mail: alberto.jimenez@icmse.csic.es

**Keywords:** luminescent, one-dimensional photonic crystals, colloidal crystal

### Abstract

Here we study the light emitted from different hybrid organic dye doped inorganic nanoparticle-based one dimensional (1D) photonic crystal (PC) architectures. The increase in the photon density of states caused by confinement in very specific slabs of the multilayer implies a lower photon group velocity,<sup>[1]</sup> which in turn yields longer light-matter interactions. We investigate both experimentally and theoretically<sup>[2]</sup> how the angular distribution of light emitted from these 1DPC structures is modified depending on the spectral matching of either resonant or stop band modes of the PC. Our measurements are explained in terms of the electromagnetic field distribution in the photonic structure. These results prove that by changing the photonic environment of a dye, it is possible to finely tune its optical response throughout the visible.

### References

- [1] Bendickson, J. M.; Dowling, J. P.; Scalora, M. *Phys. Rev. E*, **53** (1996), 4107.  
[2] Lozano, G.; Colodrero, S.; Caulier, O.; Calvo, M.E.; Míguez, H. *J. Phys. Chem. C* **114** (2010), 3681.



## **Session 3**

# **Multifunctional Nanoparticles and Nanostructures**



## Correlation lengths, porosity and water adsorption in TiO<sub>2</sub> thin films prepared by glancing angle deposition

Lola González-García<sup>1</sup>, Julián Parra-Barranco\*<sup>1</sup>,  
Juan R Sánchez-Valencia<sup>1</sup>, Ángel Barranco<sup>1</sup>, Ana Borrás<sup>1</sup>,  
Agustín R González-Elipé<sup>1</sup>, Mari-Cruz García-Gutiérrez<sup>2</sup>,  
Jaime J Hernández<sup>2</sup>, Daniel R Rueda<sup>2</sup> and Tiberio A Ezquerro<sup>2</sup>

*1 Instituto de Ciencia de Materiales de Sevilla (CSIC-Universidad de Sevilla), Avenida  
Américo Vespucio*

*49, 41092 Sevilla, Spain<sup>3</sup>*

*2 Instituto de Estructura de la Materia, CSIC, Serrano 121, 28006 Madrid, Spain*

\*contact e-mail: julian.parra@icmse.csic.es

**Keywords:** GLAD, physical vapour deposition, GISAXS, porous TiO<sub>2</sub>.

### Abstract

This work reports a thorough microstructural characterization of glancing angle deposited (GLAD) TiO<sub>2</sub> thin films. Atomic Force Microscopy (AFM), Grazing-Incidence Small-Angle X-ray Scattering (GISAXS) and water adsorption isotherms have been used to determine the evolution of porosity and the existence of some correlation distances between the nanocolumns constituting the basic elements of the film's nanostructure. It is found that the deposition angle ( $\alpha$ ) and, to a lesser extent, the film thickness are the most important parameters controlling properties of the thin film [2]. The importance of porosity and some critical dimensions encountered in the investigated GLAD thin films is highlighted in relation to the analysis of their optical properties when utilized as antireflective coatings [3] or as hosts and templates for the development of new composite materials [4].

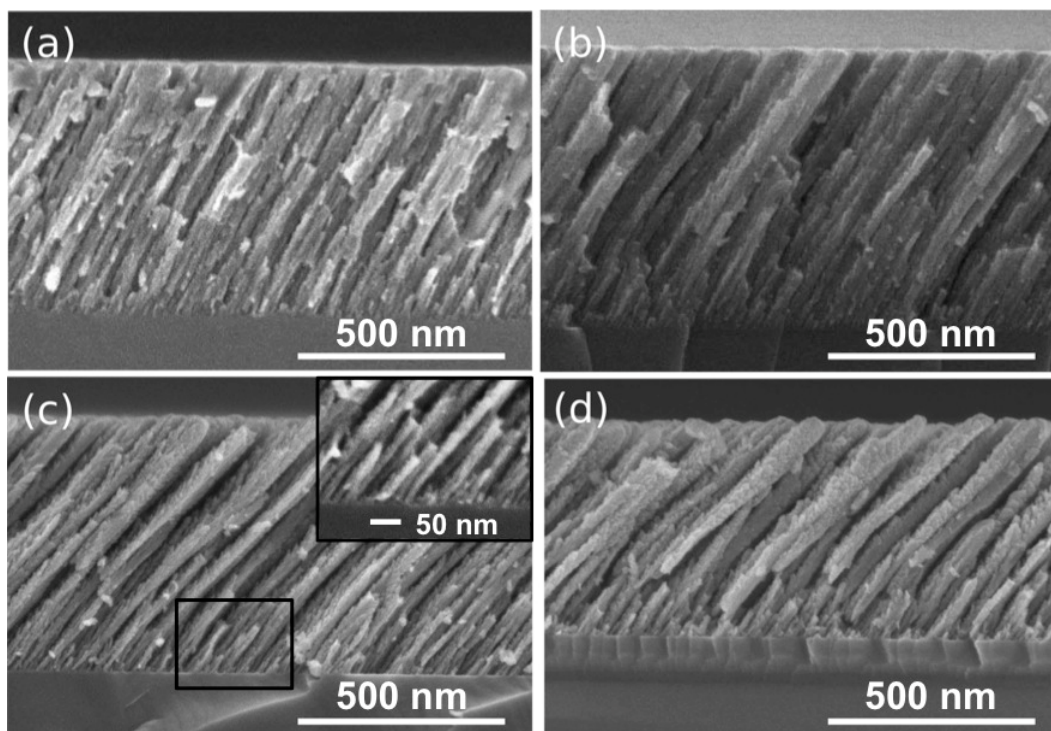


**Figure 1** – Cross-section SEM micrographs of TiO<sub>2</sub> GLAD thin films of approximately 600 nm thickness prepared at the following evaporation angles: (a) 60° (b) 70° (c) 80° and (d) 85°. The inset shows, at a higher magnification scale, the formation of thinner columns just on the substrate at the beginning of the deposition process.

### References

- [1] Hawkeye MM. and Brett MJ., *J. Vac. Sci. Technol. A.*, **25** (2007), 1317-35.
- [2] Gonzalez-Garcia L. *et al.*, *ChemPhysChem*, **11**, (2010), 2205–8.
- [3] González-García L. *et al.*, *Nanotechnology*, **23** (2012), 205701.
- [4] Sánchez-Valencia Juan R. *et al.*, *Advanced materials*, **23** (2011), 808.



## Microstructural characterization of magnetron sputtered porous silicon coatings

Jaime Caballero-Hernandez<sup>a</sup>, Vanda Godinho<sup>a\*</sup>, Roland Schierholz<sup>a</sup>, Asunción Fernández<sup>a</sup>

<sup>a</sup> *Instituto de Ciencia de Materiales de Sevilla, CSIC-Uni. Sevilla, Sevilla, Spain*

\*contact e-mail: [godinho@icmse.csic.es](mailto:godinho@icmse.csic.es)

**Keywords:** silicon porous coatings, glancing angle magnetron sputtering, closed porosity

### Abstract

Over the recent years, porous silicon has attracted considerable attention due to possible applications such as solar cells [1], optoelectronics [2] and photonic devices [3]. Being fully compatible with the established microelectronic technology, one of the most attracting features of porous silicon is its “made to order” refractive index. Recently we reported on the formation of porous silicon oxynitride coatings by magnetron sputtering with controlled refractive index depending on their deposition conditions [4,5]. The closed porosity formed allowed to keep the good mechanical and chemical properties characteristic of these coatings.

Porous silicon has been produced by a variety of approaches, but it is most commonly prepared by electrochemical etching in HF based solutions. In this work we present the possibility to produce porous silicon coatings by magnetron sputtering.

Silicon coatings with closed porosity, presenting different pore size and alignment were produced by glancing angle magnetron sputtering. The microstructure of the coatings was evaluated by scanning electron microscopy (SEM) and transmission electron microscopy (TEM), which showed clearly well-defined closed pores. (Figure 1).

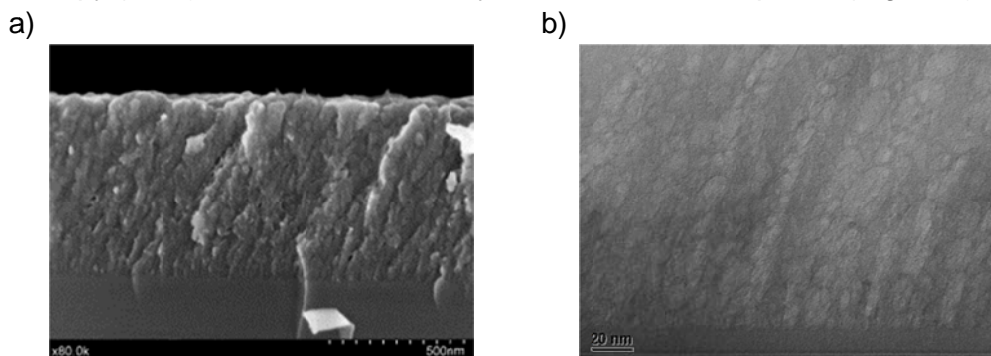


**Figure 1** – Porous silicon film deposited with helium as sputtering gas. a) Cross-sectional SEM micrograph. b) Cross-sectional TEM micrograph.

The presence of deposition gas inside the pores was proved by Rutherford backscattering spectroscopy (RBS) measurements confirming that the pores are closed and the chemical bonding state of silicon was investigated by x-ray photoelectron spectroscopy (XPS) and electron energy-loss spectroscopy (EELS). The possibility to use magnetron sputtering technique to produce different structures of alternating closed porosity with other morphologies is also explored (Figure 2).

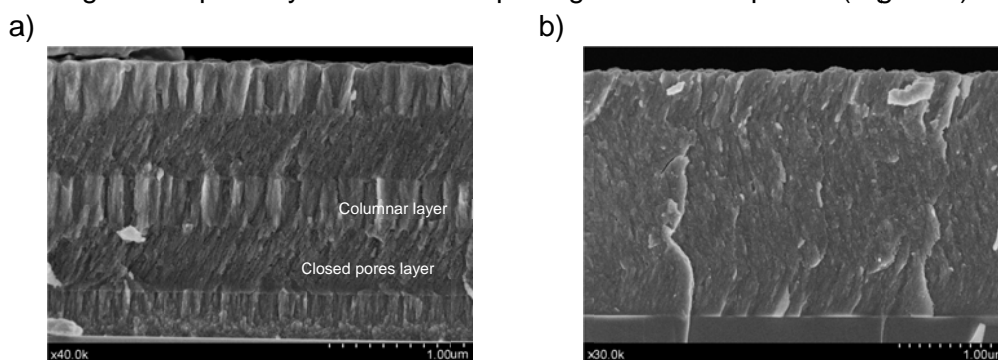


**Figure 2** – a) Multilayer alternating closed porosity and columnar layers deposited with helium and argon respectively. b) Porous coating with nanopores grown in zig-zag.

## References

- [1] A. Ramizy, Z. Hassan, K. Omar. Y. Al-Domi, M.A. Mahdi, *Applied Surface Science*, **257** (2011), 6112.
- [2] D. Abidi, S.Romdhane, A. Brunet-Burneau, J.L. Fave, *European Physical Journal Applied Physics*, **45** (2009), 10601.
- [3] R.S. Dubey, D.K. Gautam, *Optik*, **122** (2011), 494.
- [4] V.Godinho, M.C. Jiménez de Haro, J. García-López, V. Goossens, H. Terryn, M.P. Delplancke-Ogletree, A. Fernandez, *Applied Surface Science*, **256** (2010), 4548.
- [5] V. Godinho, T.C. Rojas, A. Fernandez, *Microporous and Mesoporous Materials*, **149** (2012), 142.

## Metal-ceramic materials obtained by pulsed electro-erosion treatment and magnetron sputtering for medical applications

Y.B. Solovyeva<sup>a</sup>, A.E. Kudryashov<sup>a</sup>, N.A. Gloushankova<sup>b</sup>, D.V. Shtansky<sup>a</sup>, F.V. Kiryukhantsev-Korneev<sup>a</sup>

<sup>a</sup>State Technological University, Moscow Institute of Steel and Alloys, Leninsky pr. 4, Moscow 119049, Russia

<sup>b</sup>Blokhin Cancer Research Center of RAS, Kashirskoe shosse 24, Moscow 115478, Russia

\*contact e-mail: jyisol@yandex.ru

**Keywords:** surface topography and roughness, pulse electrospark deposition, magnetron sputtering, proliferation, spreading, osseointegration.

### Abstract

Osseointegration is a key property of biomaterials intended for bone tissue substitution. The interaction between an implant and surrounding tissues is a complex dynamic process whose efficiency largely depends on the implant surface chemistry and topography. The surface treatment is an effective way to modify the surface characteristics of metal implants. In the present study, the pulsed electro-erosion treatment (PEET) was employed to change the surface topography and roughness. The PEET provides some obvious advantages such as low cost, high productivity, relative simplicity and compactness of equipment, ecological safety.

The aim of this work is to obtain metal-ceramic coating produced by PEET and magnetron sputtering methods following by the complex analyses of the structure and biocompatibility.

The deposition of coating was carried out in two steps. First, the surface of titanium substrate was modified by PEET in argon atmosphere in order to provide desired roughness, then the multicomponent bioactive nanostructured film TiCaPCON was deposited on the surface of PEET sample by magnetron sputtering of composite  $\text{TiC}_{0.5}+10\%\text{Ca}_3(\text{PO}_4)_2$  target in a gaseous mixture of  $\text{Ar}+15\%\text{N}_2$ .

For PEET, substrate material (cathode) and electrode (anode) made from Ti Grade 4 were used. The surface topography was analyzed by an optical profiling system "Wyko NT1100". The elemental composition of coatings was measured by means of glow discharge optical emission spectroscopy (GDOES) using a Profiler 2 (Horiba Jobin Yvon). XRD study was performed to assess phase composition. The bioactivity of samples *in vitro* was evaluated using MC3T3-E1 osteoblastic cells. *In vitro* studies involved the investigation of adhesion, spreading, and proliferation of MC3T3-E1 osteoblasts.

By varying the single pulse energy ( $E$ ) during PEET, materials with  $R_a=3$  (at  $E=0.025$  J) and  $R_a=8$   $\mu\text{m}$  (at  $E=0.38$  J) were obtained. The MC3T3-E1 cells on PEET-modified Ti plates coated with TiCaPCON films exhibited the morphology of well-spread polygonal cells. In the osteoblastic cells cultivated on PEET-modified samples, fluorescence staining revealed a well organized network of actin bundles (stress-fibers) terminated in large focal adhesions. The PEET surfaces were able to maintain a high level of proliferation of the cultivated osteoblastic cells. The results in-vitro experiments showed that PEET-coating with and without multicomponent nanostructured TiCaPCON films possess a high biocompatibility.

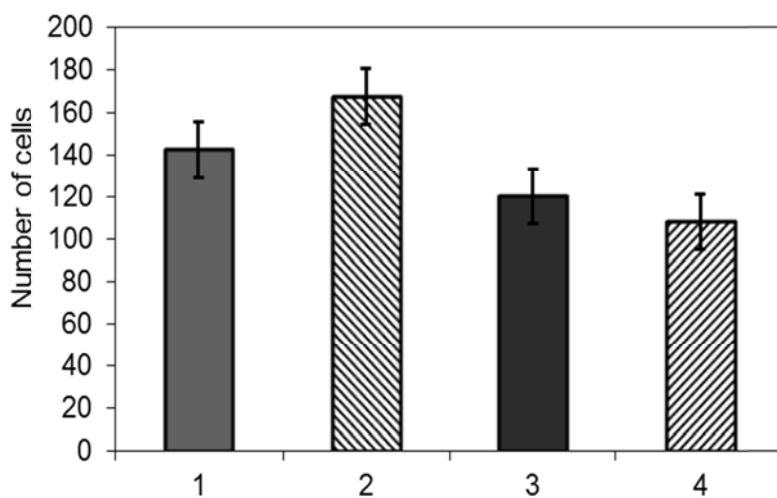


**Figure 1** - Proliferation of MC3T3-E1 osteoblasts on the surface of films. (1) PEET ( $E=0,025$  J); (2) PEET ( $E=0,025$  J) +TICAPCON film; (3) PEET ( $E=0, 38$  J); (4) PEET ( $E=0,38$  J) +TICAPCON film.

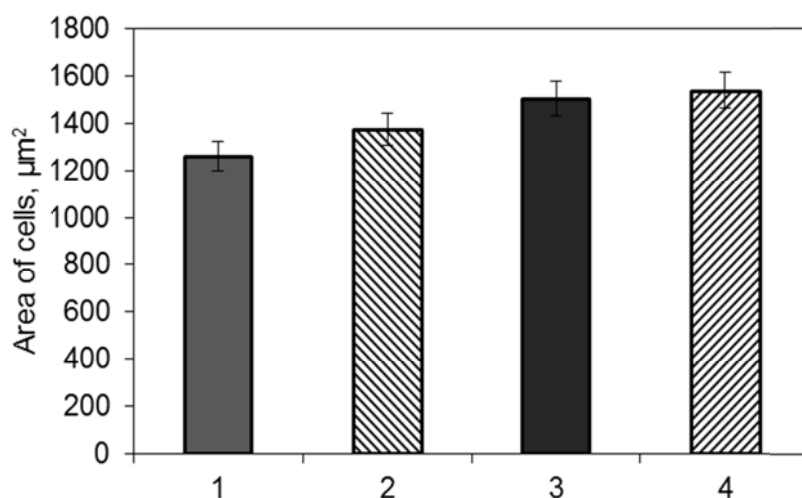


**Figure 2** - Spreading of MC3T3-E1 cells on the surface of films. (1) PEET ( $E=0,025$  J); (2) PEET ( $E=0,025$  J) +TICAPCON film; (3) PEET ( $E=0, 38$  J); (4) PEET ( $E=0,38$  J) +TICAPCON film.

## **Fabrication of the functionally graded metal-ceramic materials with controlled surface topography, chemistry, and wettability for bone substitution**

I.V. Batenina<sup>a\*</sup>, I.A. Yadroitcev<sup>b</sup>, N.S. Ryashin<sup>b</sup>, A.N. Sheveyko<sup>a</sup>, N.A. Gloushankova<sup>c</sup>,  
D.V. Shtansky<sup>a</sup>

<sup>a</sup> National University of Science and Technology "MISIS",  
Leninsky pr. 4, 164, Moscow 119049, Russia;

<sup>b</sup> Université de Lyon, Ecole Nationale d'Ingénieurs de Saint-Etienne (ENISE),  
DIPI Laboratory, 58 rue Jean Parot, 42023, Saint -Etienne Cedex 2, France

<sup>c</sup> Blokhin Cancer Research Center of RAS,  
Kashirskoe shosse 24, Moscow 115478, Russia

\*contact e-mail: irina\_bttn@mail.ru

**Keywords:** topography, wettability, biomaterials

### **Abstract**

The present work focuses on the surface modification of Ti alloys using a combination of various techniques such as cold spray (CS), selective laser sintering (SLS), and magnetron sputtering to control surface topography (roughness and blind porosity), surface chemistry, and wettability, i.e. the characteristics which affect osseointegration. The obtained results show that Ti coatings deposited by CS can be divided into three groups with a characteristic value of average roughness Ra: 4-8  $\mu\text{m}$  (single particles and agglomerates on the surface), 20-22  $\mu\text{m}$  (thin coatings), and 80  $\mu\text{m}$  (thick coatings). By varying the distance between the tracks during SLS, samples with blind porosity  $0.8\text{-}5.1 \cdot 10^{-3} \text{ mm}^3$  were obtained. In order to modify the surface chemistry, multifunctional bioactive nanostructured TiCaPCON films, 1-2  $\mu\text{m}$  thick, were deposited atop the CS, and SLS samples by sputtering a composite  $\text{TiC}_{0.5} + \text{Ca}_3(\text{PO}_4)_2$  target. The wettability measurements showed that the CS modified surfaces exhibit high values of water contact angle. TiCaPCON film deposition made the samples highly hydrophilic. The influence of the surface chemistry and surface topography on adhesion, proliferation, and early stages of osteoblasts differentiation was studied. The combination of high surface roughness and blind porosity with hydrophilicity and biocompatibility makes the fabricated metal-ceramic materials promising candidates for applications involving tissue regeneration.



## Controllable synthesis and luminescence properties of GdPO<sub>4</sub>-based nanophosphors

Ana I. Becerro<sup>\*a</sup> and M. Ocaña<sup>a</sup>

<sup>a</sup>*Instituto de Ciencia de Materiales de Sevilla (CSIC-US). c/ Américo Vespucio, 49.  
41092 Sevilla (Spain)*

\*contact e-mail: [anieto@icmse.csic.es](mailto:anieto@icmse.csic.es)

**Keywords:** GdPO<sub>4</sub>, solvothermal synthesis, luminescence properties, nanophosphors, nanoparticles.

### Abstract

There has been recently an increase research on nanostructured rare earth (RE) compounds owing to their critical importance in the fields of integrated optical systems and biomedical applications, among others [1-5]. Lanthanide orthophosphates (LnPO<sub>4</sub>) represent an important class of materials because they possess a variety of favorable thermal, chemical and optical properties. Recently, GdPO<sub>4</sub> nanoparticles have attracted much attention among other complex agents because they have shown to be efficient positive contrast agents for magnetic resonance imaging [6].

The physicochemical properties of nanomaterials are strongly associated with their size and morphology, and this applies especially to the optical properties of luminescent materials. Therefore, controlled synthesis of luminescent nanostructures with desirable size and shape is still a great challenge. Several procedures have been reported for the synthesis of GdPO<sub>4</sub> nanoparticles, most of them conducting to nanowires, nanorods [6] and nanohexagons [7].

Herein, we report the synthesis of monoclinic GdPO<sub>4</sub> particles with a new, unusual morphology consisting of three intersecting lance-shaped twins of around 500 nm long, 100 nm wide and 40 nm thick. They were synthesized in an air-force oven at 180°C using H<sub>3</sub>PO<sub>4</sub>, Gadolinium acetylacacetate and an ethylenglycol (EG)/H<sub>2</sub>O mixture as solvent. Decreasing the EG/H<sub>2</sub>O ratio leads to hexagonal rod-like particles 300 nm long x 40 nm thick. Both morphologies are maintained after doping with Eu, Tb and Dy at different levels. The twined particles show a remarkably higher luminescence compared to the rod-like ones.

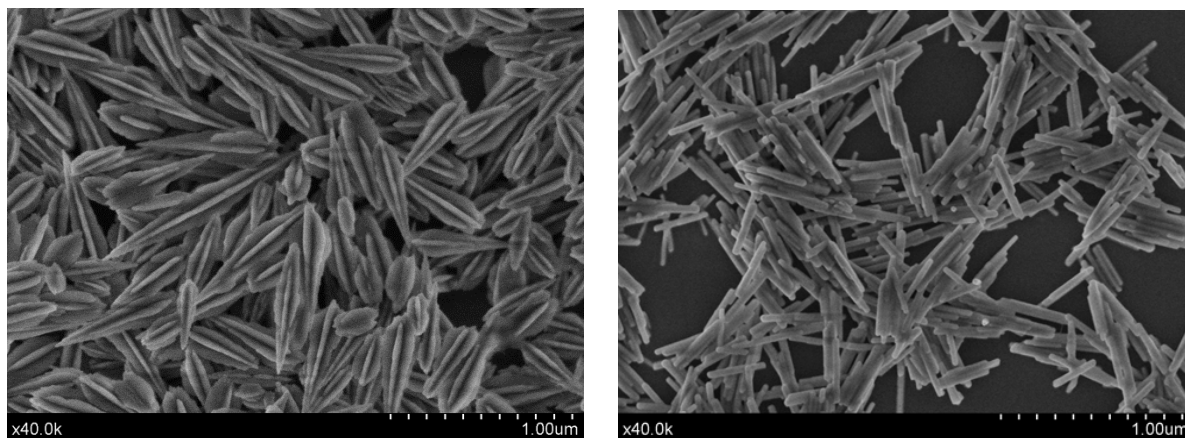


**Figure 1** – SEM photographs of lance-shaped twins and rod like GdPO<sub>4</sub> particles.

### References

- [1] Zhong, SL; Lu, Y; Gao, MR; Liu, SJ; Peng, J; Zhang, LC; Yu, SH. *Chem. A Eur. J.* **18** (2012) 5222.
- [2] Pedersen H. and Ojamae L. *Nano Lett.* **6** (2006) 2044.
- [3] Mu Q.Y.; Wang Y.D. *J. Alloys Comp.* **509** (2011) 2060.
- [4] Ocaña M., Cantelar E. and Cussó F. *Mater. Chem. Phys.* **125** (2011) 224.
- [5] Rodriguez-Liviano, S; Aparicio, FJ; Rojas, TC; Hungria, AB; Chinchilla, LE; Ocaña, M. *Cryst. Growth Design* **12** (2012) 635.
- [6] Hifumi H., Yamaoka S., Tanimoto A., Citterio D. and Suzuki K. *J. Am. Chem. Soc.* **128** (2006) 15090.
- [7] Huo, Z., Chen C., Chu D. Li H. and Li Y. *Chem. A Eur. J.* **13** (2007) 7708.



## Microwave-assisted synthesis and luminescence of mesoporous Eu-doped $\text{YPO}_4$ nanophosphors with lenticular shape

Sonia Rodriguez-Liviano,<sup>†\*</sup> Francisco J. Aparicio,<sup>†</sup> Teresa C. Rojas,<sup>†</sup> Ana B. Hungría,<sup>‡</sup> Lidia E. Chinchilla,<sup>‡</sup> Manuel Ocaña<sup>†</sup>

*<sup>†</sup>Instituto de Ciencia de Materiales de Sevilla (CSIC-UNSE), Americo Vespucio 49, Isla de La Cartuja, 41092 Sevilla, Spain.*

*<sup>‡</sup>Departamento de Ciencia de Materiales, Ingeniería Metalúrgica y Química Inorgánica. Facultad de Ciencias. Universidad de Cádiz. 11510 Puerto Real, Cádiz, Spain*

\*contact e-mail: sonia.rodriguez@icmse.csic.es

**Keywords:**  $\text{YPO}_4$ , europium, nanoparticles, mesoporous, luminescence

### Abstract

A method for the synthesis of tetragonal yttrium phosphate ( $\text{YPO}_4$ ) nanoparticles with high surface area, variable mean size, narrow size distribution and lenticular shape based on the microwave-assisted aging at low temperature (80-120°C) of ethylene glycol solutions containing only yttrium acetylacetonate and phosphoric acid is reported [1]. High Angle Annular Dark Field (HAADF) Scanning Transmission Electron Microscopy (STEM) tomography studies revealed that these lenticular nanoparticles were mesoporous whereas high resolution TEM observations indicated that they were formed through an ordered aggregation of smaller entities, which attach through their crystalline faces parallel to the *c* axis of the tetragonal structure, thus explaining their porosity and high surface area. This synthesis method is also adapted to prepare Eu-doped  $\text{YPO}_4$  red nanophosphors with morphological and structural characteristics similar to those of the undoped system, which presented high luminescence quantum efficiency. Because of their morphological, microstructural and luminescent properties as well as because of their dispersibility in water and absence of organic contamination, these nanophosphors are suitable for biomedical application (biolabelling, targeted drug delivery).

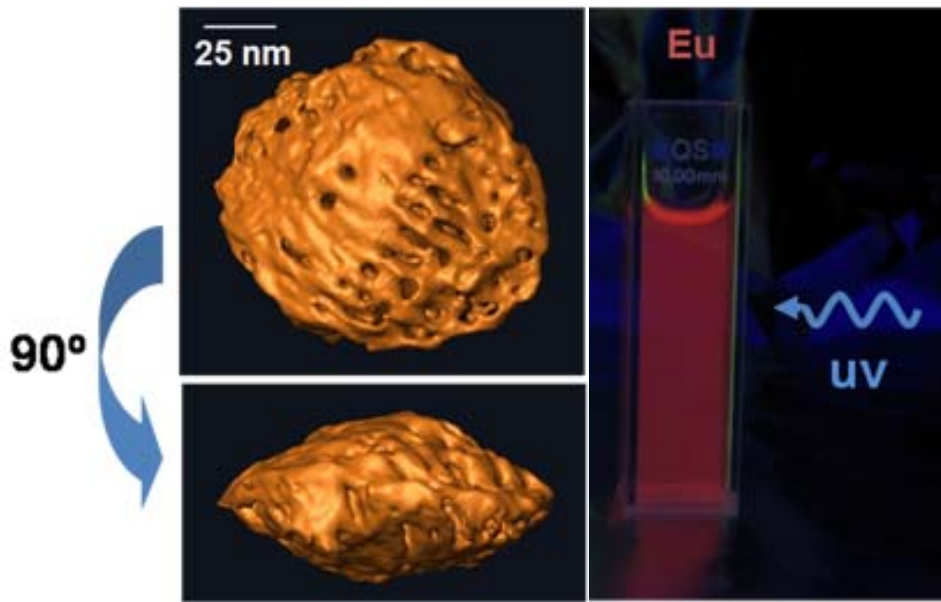


**Figure 1** – Surface rendered representations of the segmented reconstructed volume of a single nanoparticle at two different projections and photograph of the  $\text{Eu}_{0,25}\text{Y}_{0,75}\text{PO}_4$  phosphor deposited in a quartz cuvette, under UV (254nm) irradiation.

### References

- [1] Sonia Rodriguez-Liviano, Francisco J. Aparicio, Teresa C. Rojas, Ana B. Hungria, Lidia E. Chinchilla, Manuel Ocaña, *Cryst. Growth Des.*, **12**. (2012), 635-645.

## Spray pyrolysis synthesis of A-La<sub>2</sub>Si<sub>2</sub>O<sub>7</sub>: Crystal structure and luminescence

A.J. Fernández-Carrión<sup>\*a,b</sup>, M. Ocaña<sup>a</sup> and A.I. Becerro<sup>a</sup>

<sup>a</sup>*Instituto de Ciencia de Materiales de Sevilla (CSIC-US). c/ Américo Vespucio, 49.  
41092 Sevilla (Spain)*

<sup>b</sup>*Departamento de Química Inorgánica (Universidad de Sevilla), c/Profesor García-González, 1, 41071 Sevilla (Spain)*

\*contact e-mail: alberto.fernandez@icmse.csic.es

**Keywords:** La<sub>2</sub>Si<sub>2</sub>O<sub>7</sub>, pyrosilicates, spray pyrolysis, polymorphism, luminescence.

### Abstract

The optical properties of rare earth silicates have recently attracted much attention because they display an adequate behaviour for luminescent applications such as plasma displays, laser materials, and high-energy phosphors when doped with active lanthanide elements.<sup>1,2</sup> The knowledge of the luminescent properties of rare earth disilicates, RE<sub>2</sub>Si<sub>2</sub>O<sub>7</sub> (RE= lanthanides, Sc and Y) is, however, very scarce. The existing studies analyse, mainly, the behaviour of the Y<sub>2</sub>Si<sub>2</sub>O<sub>7</sub> matrix and no report has been published, to our knowledge, about the luminescent properties of La<sub>2</sub>Si<sub>2</sub>O<sub>7</sub>-based phosphors.. According to Felshe<sup>3</sup>, La<sub>2</sub>Si<sub>2</sub>O<sub>7</sub> crystallizes under two crystalline modifications: monoclinic G-La<sub>2</sub>Si<sub>2</sub>O<sub>7</sub>, with space group P2<sub>1</sub>/c, which is stable at temperatures > 1200°C and tetragonal A-La<sub>2</sub>Si<sub>2</sub>O<sub>7</sub>, with space group P4<sub>1</sub>, stable at lower temperatures. While the high T phase is easily obtained using the ceramic method at high temperature (>1500°C), the synthesis of the low T one has never been reported in the literature. This must be due to the difficulties to synthesize such a matrix as a single phase. In fact, our trials to obtain A-La<sub>2</sub>Si<sub>2</sub>O<sub>7</sub> using conventional synthesis methods as the ceramic synthesis or the sol-gel method have always been unsuccessful.

In this contribution, A-La<sub>2</sub>Si<sub>2</sub>O<sub>7</sub> was synthesised using the Spray Pyrolysis (SP) method followed by calcination at 1150 °C. The particles retained the typical spray pyrolysis spherical shape after calcination (Figure 1). The A-La<sub>2</sub>Si<sub>2</sub>O<sub>7</sub> crystal structure was described by means of XRD plus Rietveld analysis, showing 4 Si and 4 La crystallographic sites. The <sup>29</sup>Si MAS NMR spectrum of this polymorph, described for the first time in the literature, shows, in agreement with the diffraction data, 4 different Si resonances that have been ascribed to the corresponding Si sites depending on the SiOSi angle. Finally, Eu-doped A-La<sub>2</sub>Si<sub>2</sub>O<sub>7</sub> samples with different Eu contents were synthesized following the same strategy. They show a very strong red luminescence. Their

photoluminescent spectra were recorded and the Eu content that produced the optimum luminescent efficiency was established.

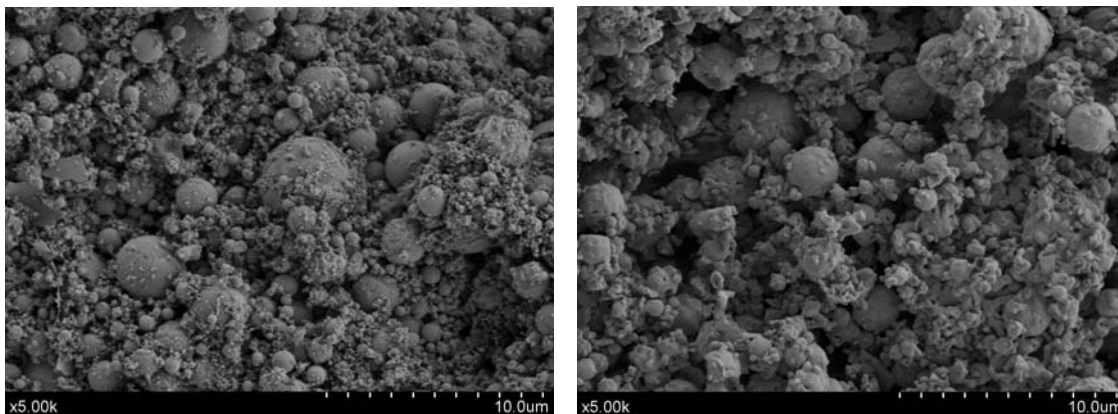


**Figure 1** – SEM micrographs of  $\text{La}_2\text{Si}_2\text{O}_7$  precursor obtained from Spray Pyrolysis (left) and the calcination product at  $1150^\circ\text{C}$  (right). The particles keep their spherical morphology after calcination, although they sinter to some degree.

### References

- [1] Díaz M., Pecharroman C., del Monte F., Sanz J., Iglesias J. E., Moyá J. S., C-Yamagata, Mello-castanho S. *Chem. Mater.* **17**, (2005), 1774-1782.
- [3] Sokolnicki, J. *J. Phys. Condens. Matter.* **22** (2010) 1-8.
- [2] Nikl M., Ren G., Ding D., Mihokova E., Jary V., Feng H. *J. Phys. Chem. Lett.* **493**, (2010), 72-75.
- [3] J. Felsche, *Struct bond*, **13** (1973), 99.

## Nanoporous-Ordered Bioactive Scaffolds for Hard Tissue Engineering

M.L. Ramiro-Gutiérrez\*<sup>a,b</sup>, A. Díaz-Cuenca\*<sup>a,b</sup>

<sup>a</sup> *Instituto de Ciencia de Materiales de Sevilla (ICMS), Centro Mixto CSIC-Universidad de Sevilla, Avda. Américo Vespucio 49, Isla de la Cartuja, 41092 Seville, Spain*

<sup>b</sup> *Networking Research Center on Bioengineering, Biomaterials and Nanomedicine (CIBER-BBN), Spain*

\* [lourdes.ramiro@icmse.csic.es](mailto:lourdes.ramiro@icmse.csic.es), [aranzazu@icmse.csic.es](mailto:aranzazu@icmse.csic.es)

**Keywords:** ordered silica, scaffolds, bioactivity, hydroxyapatite

### Abstract

Tissue engineering (TE) is an interdisciplinary field which is drawing increasing attention in materials science research with the aim to develop new and more effective biomaterials for the repair or replacement of damaged or diseased tissues. Mesoporous SBA-15 silica materials typical features, large monodisperse and tunable nanopore size (2-50 nm), very high pore volume ( $\sim 1 \text{ cm}^3 \text{ g}^{-1}$ ) and surface area ( $\sim 1000 \text{ m}^2 \text{ g}^{-1}$ ) [1], make these materials very promising for their use in drug delivery [2-4] and scaffolding in TE as they can transport large amounts of poorly soluble bioactive molecules providing increased mechanical strength and chemical stability. Besides, these materials are promising candidates as bioactive materials in bone TE [5] due to presence of silanol groups and nanoporosity which has been both reported to be crucial factors for the bioactive fixation process [6]. However, for their use in TE an important goal for these particulate precursors to be achieved, is their consolidation while preserving their nanostructural features into appropriate macroporous structures which could allow post graft vascularisation.

In this study, SBA-15 type particulate precursors have been processed successfully into macroporous scaffolds using a porogen additive, potato starch, and different processing variables. The scaffold structural and textural properties have been characterized by X-ray diffraction (SXR; WXR),  $\text{N}_2$  adsorption-desorption, nuclear magnetic resonance (RMN), infrared spectroscopy (FT-IR), field emission scanning electron microscopy (FE-SEM) and energy dispersive X-ray analysis (EDX). Also, the scaffolds bioactivity has been also monitored and correlated with their final physico-chemical parameters.

Representative FEG-SEM cross-section images of one of the consolidate materials are shown in Figure 1. The micrographs show large cavities with irregular geometries surrounded by a more dense mesoporous silica matrix. The SXR patterns of the consolidate materials maintain well resolved peaks for the main (100) reflexion and for the long order (110) and (200) reflexions confirming, after processing, the preservation of the mesostructure. In addition, areas at the scaffolds surface showing the typical flower-like crystallised calcium phosphate aggregates can be observed in Figure 1e

which are indicate of a bioactive response. The Figure 1f display their XRD analysis confirming that all the peaks matched well with those of the  $\text{Ca}_5(\text{PO}_4)_3(\text{OH})$  hydroxyapatite phase.

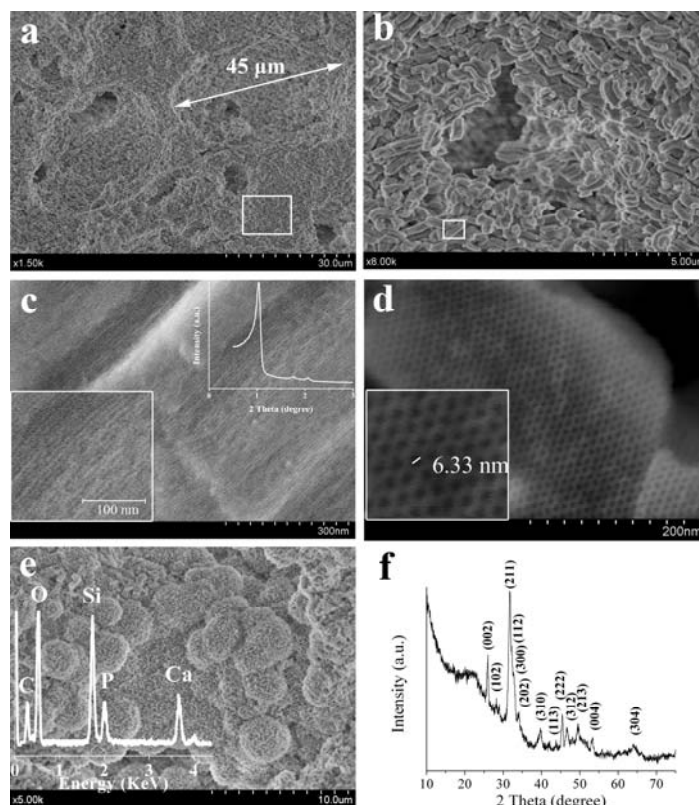


**Figure 1** – (a-d) FEG-SEM cross-section images of the consolidate material at increasing magnifications. (e) FEG-SEM micrograph and EDX analysis (inset) of the consolidate material after 28 days of soaking in SBF solution and their corresponding WXR analysis (f) showing the matching with the HA phase (JCPDS 9-432).

## References

- [1] Zhao D, Feng J, Huo Q, Melosh N, Fredrickson G.H, Chmelka B.F, Stucky G.D. *Science* **279** (1998) 548.
- [2] Wang S. *Microporous and Mesoporous Materials* **117** (2009) 1.
- [3] Doadrio A.L, Doadrio J.C, Sánchez-Montero J.M, Salinas A.J, Vallet-Regí M. *Microporous and Mesoporous Materials* **132** (2010) 559.
- [4] Al-Kady A.S, Gaber M, Hussein M.M, Ebeid E.M. *European Journal of Pharmaceutics and Biopharmaceutics* **77** (2011) 66.
- [5] Izquierdo-Barba I, Ruiz-González L, Doadrio J.C, González-Calbet J.M, Vallet-Regí M. *Solid State Sciences* **7** (2005) 983.
- [6] Kokubo T, Kim H, Kawashita M. *Biomaterials* **24** (2003) 2161.

## Biomimetic nano-mineralization of porous gelatin scaffolds for Bone Tissue-Engineering

S. Borrego-González\*<sup>a</sup>, M.L. Ramiro-Gutiérrez<sup>a, b</sup>, A. Díaz-Cuenca<sup>a, b\*</sup>

<sup>a</sup> *Instituto de Ciencia de Materiales de Sevilla (ICMS), Centro Mixto CSIC-Universidad de Sevilla, Avda. Américo Vespucio 49, Isla de la Cartuja, 41092 Seville, Spain*

<sup>b</sup> *Networking Research Center on Bioengineering, Biomaterials and Nanomedicine (CIBER-BBN), Spain*

\*[sara.borrego@icmse.csic.es](mailto:sara.borrego@icmse.csic.es) ; [aranzazu@icmse.csic.es](mailto:aranzazu@icmse.csic.es)

**Keywords:** gelatin, scaffolds, SBF, hydroxyapatite

### Abstract

The tissue engineering approach is based on the use of porous scaffolds defined as three-dimensional open-cell porous structures synthesised from either natural or synthetic materials which have the potential to support attachment, migration and multiplication of living cells (1). Ideally, scaffolds should be similar to their natural counterparts in terms of chemical composition and physical structure. In bone, the extra cellular matrix (ECM) composition is mainly collagen type I fibrils embedded with nano-sized hydroxyapatite (HA) crystals. Therefore, HA and natural polymers such as collagen or gelatin composites are materials of major interest to produce scaffolds for bone tissue-engineering (2). In the adult human bone, the HA is present as nanosized crystals of about 2–4×25×50 nm in size (3). Gelatin is a denatured form of collagen which has lost the triple-helix structure but has been proved effective to induce HA mineralization (4).

In this study, porous gelatine-mineralized scaffolds have been achieved after cross-linking, freeze-drying and a biomimetic simulated body fluid (SBF) treatment. We have studied the influence of various preparation parameters such as the gelatin concentration, the freeze-drying cooling and heating rates and their effect on the CaP mineralization. The final porous structure and the nanosized mineralized phases have been characterised using field emission scanning electron microscopy (FE-SEM), energy dispersive X-ray analysis (EDX), X-ray diffraction (XRD) and infrared spectroscopy (FTIR).

Figure 1 displays a FE-SEM micrograph and the XRD analysis of one of the obtained nanocomposites showing the presence of CaP nanocrystals. The X-ray diffraction pattern indicates the successful formation of brushite ( $\text{CaPO}_3(\text{OH}) \cdot 2\text{H}_2\text{O}$ ) (JCPDS 009-0077), and Octacalcium phosphate ( $\text{Ca}_8\text{H}_2(\text{PO}_4)_6 \cdot 5\text{H}_2\text{O}$ ) (JCPDS 026-1056) crystalline phases.

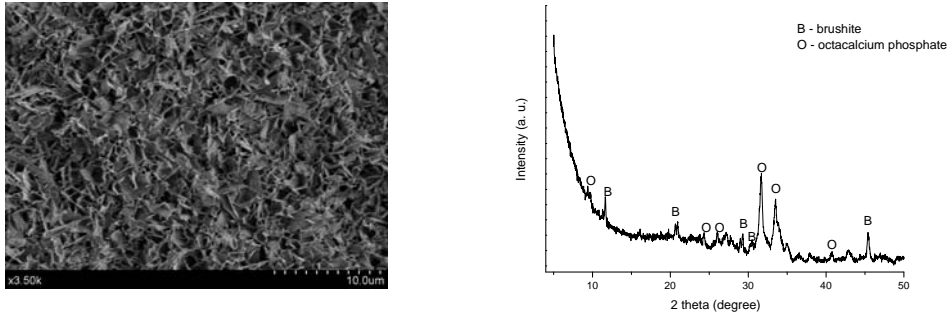


**Figure 1** – FE-SEM micrograph (left) and X-ray diffraction pattern (right) of the nanocomposite.

- [1] Yannas IV, *MIT Course*, **No: 3.961** (2006)
- [2] Knowles J, Kim H., *Journal of biomedical materials research*, **72** (2005), 136.
- [3] S.Weiner, H.D.Wagner, *Annual review of materials Science.*, **28** (1998), 271.
- [4] Azami M, Moosavifar M, Baheiraei N, Moztarzadeh F, Ai J., *Journal of biomedical materials research*, **100A**, (2012), 1347.



**Session 4**  
**Catalytic Materials**



## SYNTHESIS AND CHARACTERIZATION OF SUPPORTED Co CATALYSTS FOR HYDROGEN GENERATION BY MAGNETRON SPUTTERING

M. Paladini<sup>1\*</sup>, V. Godinho<sup>1</sup>, G.M. Arzac<sup>1</sup>, A. Fernández<sup>1</sup>

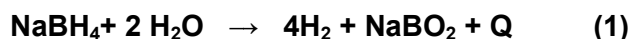
(1) Instituto de Ciencia de Materiales de Sevilla., CSIC-Univ. Sevilla. Américo Vespucio 49. Isla de la Cartuja. Seville. Spain.

(\*) contact e mail: mariana.paladini@icmse.csic.es

**Keywords:** hydrogen storage, sodium borohydride hydrolysis, Co catalyst

### Abstract

Sodium borohydride (SBH) hydrolysis is a safe reaction that permits to produce hydrogen to supply PEMFC's (Polymer Exchange Membrane Fuel Cells) for portable applications [1]



The exothermic character of the reaction permits the release of hydrogen to be carried out at ambient conditions. Basic SBH solutions are stable and only produce hydrogen when put in contact with appropriate catalysts (on demand H<sub>2</sub> generation). For the on demand production of hydrogen it is essential to prepare the catalyst in a supported form. Among catalysts, Cobalt based materials are the most investigated and the most promising candidates to replace noble metals [2].

In this work, Cobalt based materials were prepared for the first time in a supported form by magnetron sputtering as catalysts for reaction (1). This technique had proven before to be a versatile tool to prepare structured and porous materials [3]. Co catalysts were prepared under different deposition conditions and on many supports such as stainless steel, Ni foam and PTFE (Polytetrafluoroethylene) flexible membranes. The structure of these catalysts is columnar (Fig. 1). The effect of deposition conditions, nanostructure and the support itself on the catalytic activity, stability and reusability of the Cobalt catalysts was assessed.

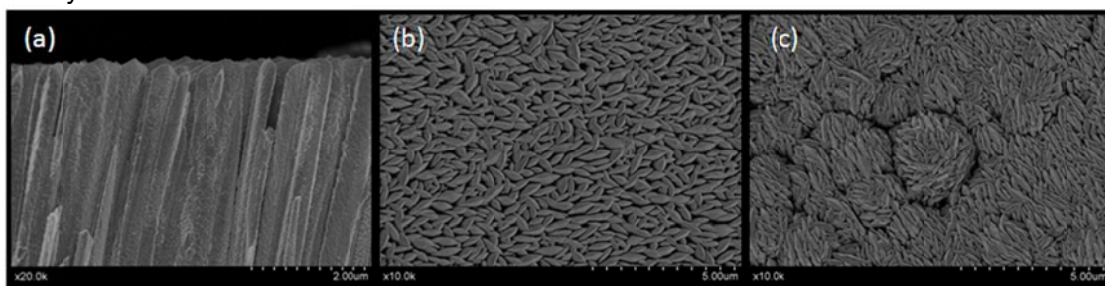


**Fig.1.** SEM micrographs of the 200W Co catalyst. Silicon supported (a) cross section (b) top view. PTFE (c) top view.

### References

[1] S.S. Muir, X. Yao, *Int J. Hydrogen Energy*, **36**,(2011), 5983-5997. References therein

- [2] U.B. Demirci, P.Miele, *Phys. Chem. ChemPhys*, **12**, (2010), 14665-14651,  
[3] V.Godinho, T.C. Rojas, A. Fernández, *Microporous and Mesoporous Materials* **148**,  
(2012) 42-146, and V.Godinho et al *J. Alloys Compd*, (2012),  
doi:10.1016/j.jallcom.2012.02.178.

